The Journal of Immunology

Innate Control of Tissue-Reparative Human Regulatory T Cells

Avery J. Lam, Katherine N. MacDonald, Anne M. Pesenacker, Stephen C. Juvet, Kimberly A. Morishita, Brian Bressler, iGenoMed Consortium, James G. Pan, Sachdev S. Sidhu, John D. Rioux and Megan K. Levings

J Immunol 2019; 202:2195-2209; Prepublished online 8 March 2019;
doi: 10.4049/jimmunol.1801330
http://www.jimmunol.org/content/202/8/2195

The Journal of Immunology is published twice each month by
The American Association of Immunologists, Inc.,
1451 Rockville Pike, Suite 650, Rockville, MD 20852

Print ISSN: 0022-1767 Online ISSN: 1550-6606.

Innate Control of Tissue-Reparative Human Regulatory T Cells

Avery J. Lam,*,† Katherine N. MacDonald,†,‡,§ Anne M. Pesenacker,*,†,1 Stephen C. Juvet,¶,‖ Kimberly A. Morishita,†,# Brian Bressler, iGenoMed Consortium,2 James G. Pan,†† Sachdev S. Sidhu,††,‡‡ John D. Rioux,§§,¶¶ and Megan K. Levings*,†,‡**

Regulatory T cell (Treg) therapy is a potential curative approach for a variety of immune-mediated conditions, including autoimmunity and transplantation, in which there is pathological tissue damage. In mice, IL-33R (ST2)–expressing Tregs mediate tissue repair by producing the growth factor amphiregulin, but whether similar tissue-reparative Tregs exist in humans remains unclear. We show that human Tregs in blood and multiple tissue types produced amphiregulin, but this was neither a unique feature of Tregs nor selectively upregulated in tissues. Human Tregs in blood, tonsil, synovial fluid, colon, and lung tissues did not express ST2, so $ST2^+$ Tregs were engineered via lentiviral-mediated overexpression, and their therapeutic potential for cell therapy was examined. Engineered $ST2^+$ Tregs exhibited TCR-independent, IL-33–stimulated amphiregulin expression and a heightened ability to induce M2-like macrophages. The finding that amphiregulin-producing Tregs have a noneffector phenotype and are progressively lost upon TCR-induced proliferation and differentiation suggests that the tissue repair capacity of human Tregs may be an innate function that operates independently from their classical suppressive function. ***The Journal of Immunology*****, 2019, 202: 2195–2209.**

Cell therapy with regulatory T cells (Tregs) holds significant promise as a potential curative approach for a variety of immune-mediated conditions, from autoimmunity to transplant rejection. Tregs normally suppress the activation and effector function of other immune cells to maintain self-tolerance and homeostasis, and adoptive transfer of ex vivo–expanded Tregs has been found to be safe and potentially efficacious in clinical trials for graft-versus-host disease and type 1 diabetes (1). Although the majority of research on Treg biology to date has centered on their immunosuppressive potential, there has been an increasing appreciation for the nonimmune functions of Tregs, particularly in tissue-specific contexts (2, 3).

Several reports in mice have shown that Tregs participate in tissue repair (reviewed in Refs. 2, 4). In models of muscle and skin injury, Tregs indirectly facilitate wound healing by limiting IFN-γ production and promoting anti-inflammatory myeloid cells (5–8). Mouse Tregs also act directly on parenchymal cells to drive repair: muscle- and lung-infiltrating Tregs mediate muscle and lung repair after injury or influenza infection, respectively, via production of amphiregulin (AREG), a low-affinity EGFR ligand (5, 9). In muscles, AREG induces satellite cell differentiation in vitro, and its administration to injured mice improves muscle repair (5). In a model of influenza-induced lung damage, the early production of Treg-derived AREG was found to be critical for normal tissue

*Department of Surgery, University of British Columbia, Vancouver, British Columbia V5Z 4H4, Canada; †BC Children's Hospital Research Institute, Vancouver, British Columbia V5Z 4H4, Canada; ‡School of Biomedical Engineering, University of British Columbia, Vancouver, British Columbia V6T 1Z4, Canada; §Michael Smith Laboratories, University of British Columbia, Vancouver, British Columbia V6T 1Z4, Canada; ¶Division of Respirology, Department of Medicine, University of Toronto, Toronto, Ontario M5G 2C4, Canada; ‖Toronto General Hospital Research Institute, University Health Network, Toronto, Ontario M5G 2C4, Canada; #Division of Rheumatology, Department of Pediatrics, University of British Columbia, Vancouver, British Columbia V5Z 4H4, Canada; **Division of Gastroenterology, Department of Medicine, University of British Columbia, Vancouver, British Columbia V6Z 1Y6, Canada; ††Toronto Recombinant Antibody Centre, Donnelly Centre for Cellular and Biomolecular Research, University of Toronto, Toronto, Ontario M5S 3E1, Canada; ‡‡Department of Molecular Genetics, University of Toronto, Toronto, Ontario M5S 1A8, Canada; §§Department of Biochemistry and Molecular Medicine, University of Montreal, Montreal, Quebec H3T 1J4, Canada; and ¶¶Montreal Heart Institute, Montreal, Quebec H1T 1C8, Canada

[1]Current address: Division of Infection and Immunity, Institute of Immunity and Transplantation, University College London, London, U.K.

[2]All authors and their affiliations appear at the end of the article.

ORCIDs: 0000-0001-7794-1325 (A.J.L.); 0000-0003-4883-2757 (K.N.M.); 0000-0002-7968-0277 (A.M.P.); 0000-0002-7243-556X (S.C.J.); 0000-0002-1389-4002 (K.A.M.); 0000-0002-7144-726X (J.G.P.); 0000-0001-7755-5918 (S.S.S.); 0000-0001-7560-8326 (J.D.R.); 0000-0002-0305-5790 (M.K.L.).

Received for publication October 1, 2018. Accepted for publication January 23, 2019.

This work was supported by grants from the Canadian Institutes of Health Research (FDN-154304 to M.K.L.) and the iGenoMed Consortium, which receives financial support from Génome Québec, Genome Canada, the Government of Canada, the Ministère de l'Enseignement Supérieur, de la Recherche, de la Science et de la Technologie du Québec, the Canadian Institutes of Health Research (with contributions from the Institute of Infection and Immunity, the Institute of Genetics, and the Institute of Nutrition, Metabolism and Diabetes), Genome British Columbia, Crohn's Colitis Canada, and Agilent Technologies. A.J.L. is supported by a Canadian Institutes of Health Research doctoral award, K.N.M. is supported by a BC Children's Hospital Research Institute graduate award, A.M.P. is supported by a Juvenile Diabetes Research Foundation postdoctoral fellowship and an Arthritis Research UK career development fellowship, and M.K.L. receives a salary award from the BC Children's Hospital Research Institute.

Conceptualization: A.J.L. and M.K.L. Methodology: A.J.L., K.N.M., A.M.P., and M.K.L. Investigation: A.J.L. Resources: K.N.M., A.M.P., S.C.J., K.A.M., B.B., J.G.P., and S.S.S. Writing—original draft: A.J.L. and M.K.L. Writing—review and editing: A.J.L., A.M.P., S.C.J., J.D.R., and M.K.L. Supervision: M.K.L. Funding acquisition: iGenoMed Consortium, J.D.R., and M.K.L.

The sequences presented in this article have been submitted to the Gene Expression Omnibus (https://www.ncbi.nlm.nih.gov/geo/) under accession number GSE117481.

Address correspondence and reprint requests to Dr. Megan K. Levings, University of British Columbia, 950 West 28th Avenue, Room A4-186, Vancouver, BC V5Z 4H4, Canada. E-mail address: mlevings@bcchr.ca

The online version of this article contains supplemental material.

Abbreviations used in this article: AREG, amphiregulin; CPD, cell proliferation dye; ILC2, type 2 innate lymphoid cell; moDC, monocyte-derived dendritic cell; NGFR, nerve growth factor receptor; NGFR Treg, NGFR-transduced Treg; ST2 Treg, ST2–NGFR–transduced Treg; Tconv, conventional T cell; Treg, regulatory T cell.

repair (9). Tissue-reparative mouse Tregs also have distinct features, including a highly activated phenotype and a unique gene signature, which is likely imprinted locally. Notably, these cells seem to be recruited from the circulation, as their accumulation in injured skin and muscle is reduced upon blockade of lymphocyte egress from lymphoid organs (7, 10).

Accumulating evidence in mice suggests that IL-33 has an important role in promoting tissue-specific Treg activation and repair function. Specifically, upon injury or necrosis, epithelial barrier tissues release IL-33, which acts on IL-33R (ST2; *IL1RL1*)–expressing cells, including $ST2^+$ tissue-reparative Tregs in the muscle and lung (5, 9, 10). In vitro, IL-33 induces AREG production by mouse $ST2^+$ Tregs (9) and in vivo can recruit Tregs to initiate muscle regeneration (10). Furthermore, IL-33 maintains *Areg*-expressing, $ST2^+$ Tregs in multiple nonlymphoid tissues, including the colon, muscle, and visceral adipose tissue (10–13), in part through GATA3-mediated reinforcement of ST2 and FOXP3 expression (12, 14). $ST2^+$ Tregs are also poised to suppress the inflammatory effects of IL-33 release: $ST2^+$ Tregs in IL-33–treated mice potently suppress IL-33–augmented IFN-γ production by $CD8^+$ and $CD4^+$ T cells (15, 16), and in a mouse model of allogeneic stem cell transplantation, IL-33–expanded $ST2^+$ Tregs protect mice from IL-33–mediated rejection (17). Collectively, these studies underpin the importance of the IL-33/ST2 and/or AREG pathways in mediating the tissue-reparative capacity of mouse Tregs in a variety of contexts.

In this study, we aimed to answer the outstanding question of whether human Tregs have a similar tissue repair potential. There are limited data on whether human $ST2^+$ Tregs are present in various tissues (18, 19). Also unknown is whether human Tregs have the potential to produce AREG in response to IL-33 or other factors, although human $CD4^+$ T cells have been described to produce AREG in response to TCR activation (20). Given the potential therapeutic advantage of using tissue-reparative Tregs in numerous cell therapy applications, we investigated sources of therapeutic ST2-expressing human Tregs and explored their biological properties.

Materials and Methods

Cell isolation and culture from human blood and tissue specimens

Human samples were collected with written informed consent, and collection was performed according to protocols approved by the University of British Columbia Clinical Research Ethics Board, the Canadian Blood Services Research Ethics Board, and the University Health Network Research Ethics Board. PBMCs from healthy adults were isolated via Lymphoprep (STEMCELL Technologies). For Treg isolation, $CD4^+$ and $CD25^+$ cells were sequentially enriched with a RosetteSep $CD4^+$ T Cell Enrichment Cocktail (STEMCELL Technologies) and CD25 MicroBeads II (Miltenyi Biotec) before flow sorting on a FACSAria IIU (BD Biosciences) or MoFlo Astrios (Beckman Coulter). Total Tregs and total conventional T cells (Tconvs) were sorted as $CD4^+CD25^{hi}CD127^{lo}$ and $CD4^+CD25^{lo}CD127^{hi}$, respectively; naive Tregs and naive Tconvs were sorted as $CD4^+CD25^{hi}CD127^{lo}CD45RA^+$ and $CD4^+CD25^{lo}CD127^{hi}CD45RA^+$, respectively. $CD3^+$ T cells and type 2 innate lymphoid cells (ILC2s) were isolated by negative selection; $CD14^+$ monocytes were isolated by positive selection (all STEMCELL Technologies).

Tonsil tissues removed from healthy children were cut into small pieces, and mononuclear cells were isolated by Lymphoprep. Synovial fluid from joints affected by juvenile idiopathic arthritis was first incubated with hyaluronidase (10 IU/ml; Sigma-Aldrich) for 20 min at 37˚C before mononuclear-cell isolation with Lymphoprep. Lamina propria mononuclear cells were isolated from colon biopsy specimens from subjects undergoing colon cancer screening by digestion with collagenase VIII (100 IU/ml) and DNase IV (150 μg/ml; both Sigma-Aldrich) for 1 h at 37˚C, and mononuclear cells were isolated with a 40/80% Percoll gradient (GE Healthcare) (21). Noncancerous lung tissue from patients with lung tumors undergoing resection was cut into small pieces and digested with collagenase A (1 mg/ml; Sigma-Aldrich) and DNase I (200 μg/ml; Sigma-Aldrich) in a gentleMACS Dissociator (37C_m_LDK_1 program; Miltenyi Biotec); RBCs were removed by incubation with a hypotonic solution (15 mM NH_4Cl, 10 mM $KHCO_3$, and 70 μM EDTA) for 5 min at room temperature.

Unless otherwise specified, all cells were cultured at 37˚C and 5% CO_2 in X-VIVO 15 (Lonza) supplemented with 5% (v/v) human serum (WISENT), 1% (v/v) penicillin–streptomycin (Life Technologies), 2 mM GlutaMAX (Life Technologies), and phenol red (Sigma-Aldrich). During the differentiation of monocyte-derived dendritic cells (moDCs), the medium above was additionally supplemented with 1 mM sodium pyruvate (STEMCELL Technologies).

Naive Treg expansion and transduction

Flow-sorted naive Tregs or naive Tconvs were stimulated 1:1 with 75-Gy–irradiated artificial APCs expressing CD32, CD52, and CD80 (22) in the presence of OKT3 (0.1 μg/ml; University of British Columbia Ab Lab) and IL-2 (1000 IU/ml for Tregs, 100 IU/ml for Tconvs). Cells were transduced with a bidirectional-promoter lentiviral vector encoding ST2 and a truncated nerve growth factor receptor (NGFR) or NGFR only (multiplicity of infection = 10) 1 d later. Media and IL-2 were refreshed every 2–3 d. On day 7 of expansion, $NGFR^+$ cells were bead-purified by positive selection (Miltenyi Biotec) and restimulated with artificial APCs, OKT3, and IL-2 as described above. In some cases, IL-33 (20 ng/ml; BioLegend) was added on days 7, 9, and 11 of expansion. Cell viability on day 12 was determined by ViaStain Acridine Orange/Propdium Iodide Staining Solution (Nexcelom). All cells were collected on day 12 and rested overnight in reduced IL-2 (100 IU/ml for Tregs, none for Tconvs) before functional assays.

Polyclonal Treg coculture with moDCs

$CD14^+$ monocytes were differentiated into moDCs for 7 d with GM-CSF (50 ng/ml) and IL-4 (100 ng/ml; both STEMCELL Technologies); media and cytokines were refreshed every 2–3 d. Maturation was induced by a combination of IL-1β (10 ng/ml; Invitrogen), IL-6 (100 ng/ml; Invitrogen), TNF-α (10 ng/ml; Invitrogen), PGE2 (1 μg/ml; Tocris) (all last 2 d), and IFN-γ (50 ng/ml; Invitrogen) (last 1 d). Maturation was confirmed via flow cytometry by high expression of CD80, CD83, CD86, and HLA-DR. Flow-sorted total Tregs were cocultured 1:1 with 50-Gy–irradiated moDCs, OKT3 (1 μg/ml), and IL-2 (1000 IU/ml). Media and IL-2 were refreshed every 2–3 d. IL-33 (20 ng/ml) was added on days 0, 3, 5, 7, 9, and 11 of Treg:moDC coculture. All cells were collected on day 12 and rested overnight in reduced IL-2 (100 IU/ml) before phenotypic analysis.

Development and validation of anti-human ST2 mAbs

For selection of phage-displayed anti-human ST2 Abs, the human ST2 extracellular domain was fused to a human Fc region, and the resulting protein was expressed in HEK-293 cells, purified, and used as the Ag to screen against a synthetic phage-displayed Fab library. Fabs that bound specifically to the human ST2 extracellular domain but not human Fc were selected, fused to a mouse IgG2a C region, expressed, purified from HEK-293 cells, and used for in vitro testing (23).

For in vitro testing, HEK-293T cells were transiently transfected with a vector encoding ST2–GFP or IL-1RAP–GFP using Lipofectamine 3000 (Invitrogen) according to the manufacturer's protocol, and ST2 expression was assessed after 1 d with the indicated mAbs. To generate ST2-transduced primary human T cells for mAb validation, CD4-enriched PBMCs were transduced with a lentiviral vector encoding ST2–NGFR and expanded for 7 d with artificial APCs, OKT3, and IL-2 as described above. ST2 expression was assessed after expansion with the indicated Abs.

Assessment of proliferation, AREG expression, and cytokine secretion

Tregs or Tconvs (either ex vivo–sorted total Tregs/Tconvs or expanded naive Tregs/Tconvs) were activated with IL-2 (100 IU/ml) and anti-CD3/CD28–coated beads (Life Technologies Dynabeads T-Expander; 1:1 bead/cell) in the presence or absence of IL-18 (MBL International) and/or IL-33 (20 ng/ml each). In some cases, cells were first labeled with cell proliferation dye (CPD; Invitrogen) according to the manufacturer's protocol before activation; proliferation was determined after 4 d by CPD dilution via flow cytometry.

For *AREG* mRNA expression, cells were lysed at the indicated times. Supernatants were collected after 4 d for detection of secreted cytokines, including AREG. For flow cytometric detection of AREG protein, cells were restimulated with PMA (10 ng/ml), ionomycin (500 μg/ml), and brefeldin A (10 μg/ml; all Sigma-Aldrich) for an additional 4 h. To assess

AREG production potential ex vivo by flow cytometry, cells were activated with PMA, ionomycin, and brefeldin A as described above.

Concentrations of AREG in supernatants were determined by ELISA (R&D Systems DuoSet ELISA) according to the manufacturer's protocol. Concentrations of CCL3, CCL4, CCL5, GM-CSF, IFN-γ, IL-2, IL-4, IL-8, IL-10, IL-13, IL-17A, IL-22, and TNF-α were assessed by cytometric bead array (BioLegend custom LEGENDplex 13-plex kit) and analyzed by LEGENDplex software (v7.1; BioLegend) according to the manufacturer's protocols.

T cell suppression and monocyte alternative activation assays

For T cell suppression, expanded naive Tregs and ex vivo–isolated allogeneic $CD3^+$ T cells (responder cells) were differentially labeled with CPD, cocultured at the indicated ratios, and activated with anti-CD3/CD28–coated beads (1:16 beads/responder cells) and IL-33 (20 ng/ml) for 4 d. Proliferation of $CD4^+$ and $CD8^+$ cells within the responder cell fraction was determined by CPD dilution. Responder cells activated alone with beads (±IL-33) served as positive controls. Percent suppression of proliferation was calculated as: (1 − [percent divided of sample/percent divided of positive control]) × 100.

For monocyte alternative activation, expanded naive Tregs and freshly isolated allogeneic $CD14^+$ monocytes were cocultured at the indicated ratios and activated with IL-2 (100 IU/ml), OKT3 (1 μg/ml), and IL-33 (20 ng/ml) for 40 h. Monocytes activated alone with IL-2 and OKT3 (±IL-33) served as positive controls. Cells were detached by incubation with ice-cold PBS with 5 mM EDTA for 20 min on ice and then collected for flow cytometric analysis.

Quantitative PCR

Cells were lysed, total RNA was extracted, and cDNA was synthesized using a Total RNA Mini Kit (Geneaid) and qScript cDNA SuperMix (Quantabio) according to the manufacturers' protocols. Quantitative PCR was set up with PerfeCTa SYBR Green FastMix (Quantabio) and performed on a ViiA 7 Real-Time PCR System (Applied Biosystems). The relative expression of each gene was normalized to the housekeeping genes *RPL13A* and *SDHA* by the comparative threshold cycle method using QuantStudio software (v1.3; Applied Biosystems). Primer sequences (Invitrogen): *AREG* forward, 5′-GGTGGTGCTGTCGCTCTTGA-3′; *AREG* reverse, 5′-AATCCATCAGCACTGTGGTCCC-3′; *RPL13A* forward, 5′-CTCAAGGTCGTGCGTCTGAA-3′; *RPL13A* reverse; 5′-CTGTCACTGCCTGGTACTTCCA-3′; *SDHA* forward, 5′-ACTCAGCATGCAGAAGTCAATGC-3′; *SDHA* reverse, 5′-ACCTTCTTGCAACACGCTTCCC-3′.

RNA sequencing and data analysis

Expanded naive Tregs were activated with IL-2 (100 IU/ml) and 1:1 anti-CD3/CD28–coated beads in the presence or absence of IL-33 (20 ng/ml) for 16 h. Total RNA was isolated using RNAzol RT (Sigma-Aldrich). RNA quality was assessed by an Agilent Bioanalyzer 2100 and an RNA 6000 Nano Kit (Agilent Technologies); all samples used in this study had an RNA integrity number of 9.8–10. mRNA enrichment and library preparations were performed with a NEBNext Poly(A) mRNA Magnetic Isolation Module and a NEBNext Ultra II Directional RNA Library Prep Kit for Illumina (both New England Biolabs). Paired-end libraries were sequenced (43 × 43 bp reads) on a NextSeq 500 (Illumina). Read sequences were aligned to the GRCh37/hg19 reference genome using STAR (v2.5.0a), and Illumina's RnaReadCounter tool was used for quantification of gene expression; >8 reads across each of eight samples was considered detectable.

Differentially expressed genes were identified by pairwise comparisons using DESeq2 (v1.16.1) (24) within the R statistical environment (v3.4.2). For gene set enrichment analysis, all detectable genes were ranked using the following metric: sign($\log_2$[fold change]) × $-\log_{10}(p$ value). The ranked list was compared with the Molecular Signatures Database gene set collections, including Hallmark (v6.1; Broad Institute), using the GSEAPreranked tool in Gene Set Enrichment Analysis software (v3.0; Broad Institute) (25) with default settings and the classic Kolmogorov–Smirnov statistic. Data were deposited within the National Center for Biotechnology Information Gene Expression Omnibus (https://www.ncbi.nlm.nih.gov/geo/) under accession number GSE117481.

Flow cytometry

Commercial Abs and dyes can be found in Supplemental Table I. Cells were stained for surface proteins in PBS or Brilliant Stain Buffer (BD Biosciences) for 20 min at room temperature; fixable viability dye (Invitrogen) was used to exclude dead cells. In experiments involving PBMCs or tissue samples, cells were preincubated with human Fc receptor binding inhibitor (Invitrogen) for 10 min at 4°C. For intracellular proteins, cells were fixed and permeabilized with the eBioscience Foxp3/Transcription Factor Staining Buffer Set (Invitrogen) following the manufacturer's protocol.

For intracellular cytokine staining, cells were activated with PMA, ionomycin, and brefeldin A for 4 h as described above. AREG expression was revealed with fluorochrome-conjugated streptavidin. For assessment of ST2 expression on blood- and tissue-derived samples, cells were either stained directly or first cultured with IL-2 (100 IU/ml) and IL-33 (50 ng/ml) for 24 h as indicated. For signal transduction, cells were rested overnight without human serum or IL-2 and then activated with IL-33 (50 ng/ml) for the indicated times at 37°C while shaking (900 rpm), fixed and permeabilized with Cytofix and Perm Buffer III buffers (both BD Biosciences) according to the manufacturer's protocol, and stained for phospho-proteins.

All samples were acquired on an LSRFortessa X-20 (BD Biosciences) or Cytoflex (Beckman Coulter), and data were analyzed with FlowJo software (v10.4; Tree Star).

Statistical analysis

Statistical significance was determined by Wilcoxon matched-pairs signed-rank test, Friedman or Kruskal–Wallis test with Dunn multiple comparisons test, or matched two-way ANOVA with Tukey, Dunnett, or Sidak multiple comparisons tests, as appropriate. The *n* values used to calculate statistics are defined in the figure legends; significance ($p < 0.05$ was considered significant) is indicated within the figures. Analysis was performed using Prism 7 software (GraphPad; v7.0d).

Results

Human AREG-producing Tregs from blood and tissues have a noneffector phenotype

In mice, Treg production of AREG is restricted to cells with an effector memory ($CD44^{hi}CD62L^{lo}$) phenotype (9). We first characterized the ability of human Tregs from blood, lymphoid, and nonlymphoid tissues to produce AREG. In blood, we found that a proportion of Tregs (gated as $CD4^+CD25^{hi}FOXP3^+$) produced AREG ex vivo but at a significantly lower frequency than Tconvs ($CD4^+CD25^{lo}FOXP3^-$) (Fig. 1A). As AREG mediates its tissue-reparative effects by acting directly on parenchymal cells, we hypothesized that a larger fraction of Tregs in nonlymphoid tissues may be poised to produce AREG. Thus, we obtained samples of normal human tonsil, colon, and lung tissues, as well as synovial fluid from patients with juvenile idiopathic arthritis. In all tissues examined, a subset of Tregs produced AREG ex vivo, but the highest frequency of $AREG^+$ Tregs was found in blood rather than tissues (Fig. 1B). Surprisingly, and in contrast to reports from mice, AREG-producing Tregs were enriched for a naive, noneffector phenotype. AREG expression was found mainly in the $HLA\text{-}DR^-$ fraction of Tregs in blood and across multiple tissue types (Fig. 1B).

Predominant expression of AREG by noneffector Tregs persisted after TCR activation. Blood Tregs were sorted ($CD4^+CD25^{hi}CD127^{lo}$) and TCR-activated for 4 d; the majority of AREG-expressing Tregs were present in $HLA\text{-}DR^-$ Tregs rather than $HLA\text{-}DR^+$ Tregs (Fig. 2A). Similar results were found after TCR activation of sorted $HLA\text{-}DR^+$ and $HLA\text{-}DR^-$ Tregs (Fig. 2B).

Compared to their $AREG^-$ counterparts, AREG-producing Tregs ex vivo had consistently lower expression of CD39, CCR4, Helios, HLA-DR, and TIGIT (Fig. 2C)—proteins associated with Treg activation and/or effector function (22, 26–29). Furthermore, using CCR7 and CD45RA to define Treg differentiation status, we found a progressive decline in ex vivo AREG production potential as Tregs transitioned from naive ($CD45RA^+CCR7^+$) to central memory ($CD45RA^-CCR7^+$) and effector memory ($CD45RA^+CCR7^-$) (Fig. 2D). Similarly, $AREG^+$ Tregs were enriched for a naive phenotype rather than an effector memory phenotype (Fig. 2E). Overall, AREG expression by human Tregs in both blood and tissues is associated with a noneffector Treg phenotype.

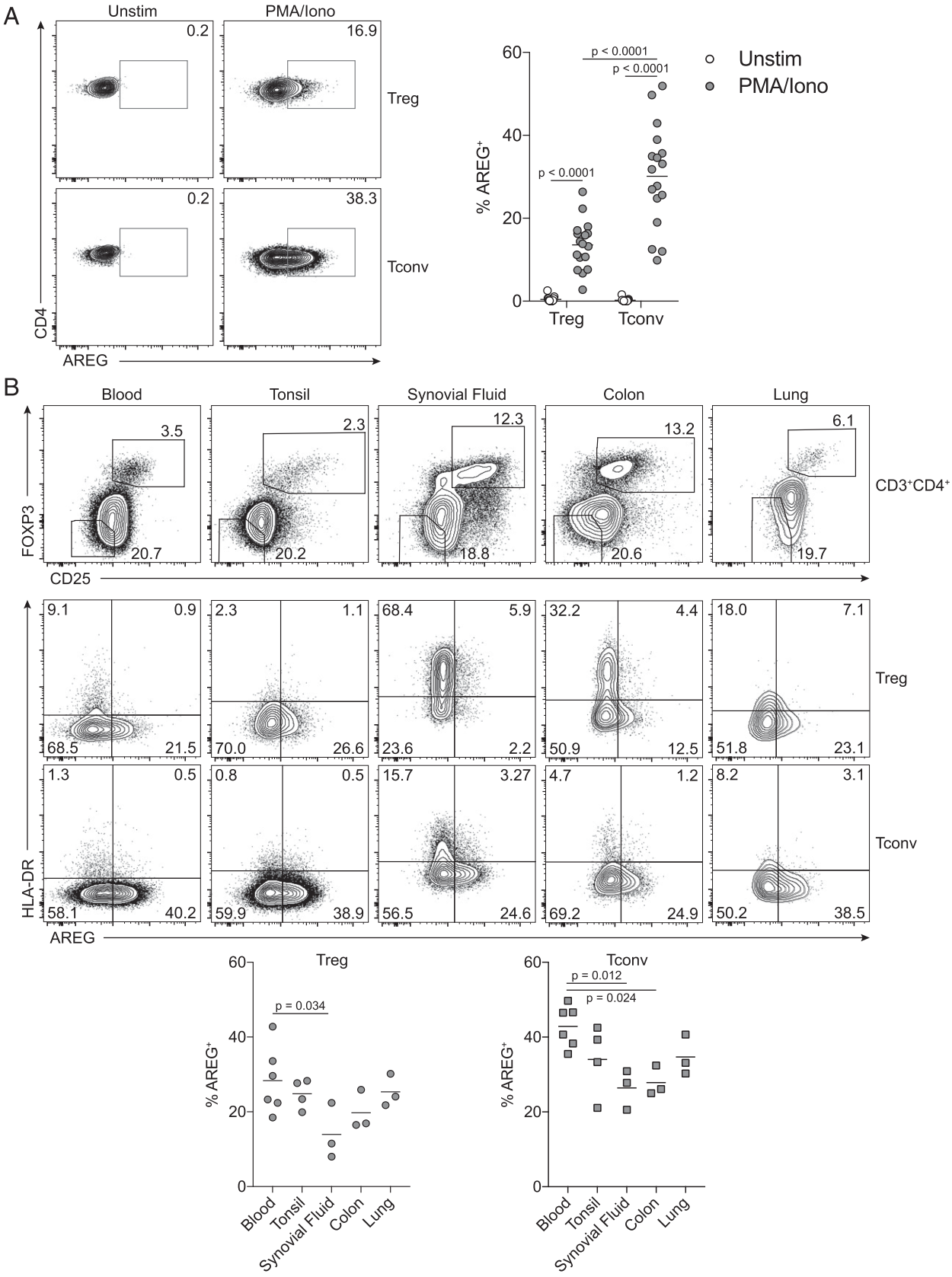

FIGURE 1. Human Tregs from blood and multiple tissue types can produce AREG. (**A**) CD4-enriched PBMCs were activated with PMA, ionomycin, and brefeldin A (PMA/Iono; 4 h) or left unstimulated in the presence of brefeldin A (Unstim; 4 h). AREG expression (left, representative; right, $n = 17$) was quantified within gated Tregs ($CD4^+CD25^{hi}FOXP3^+$) and Tconvs ($CD4^+CD25^{lo}FOXP3^-$). (**B**) Mononuclear cells from blood ($n = 6$), tonsil ($n = 4$), synovial fluid ($n = 3$), colon ($n = 3$), and lung tissue ($n = 3$) were activated as in (A). AREG expression was determined in Tregs ($CD4^+CD25^{hi}FOXP3^+$) and Tconvs ($CD4^+CD25^{lo}FOXP3^-$). Representative Treg and Tconv gates within $CD3^+CD4^+$ T cells (top), representative AREG expression in Tregs and Tconvs (middle), and quantification (bottom). Significance for (A) and (B) was determined by matched two-way ANOVA with Tukey multiple comparisons test.

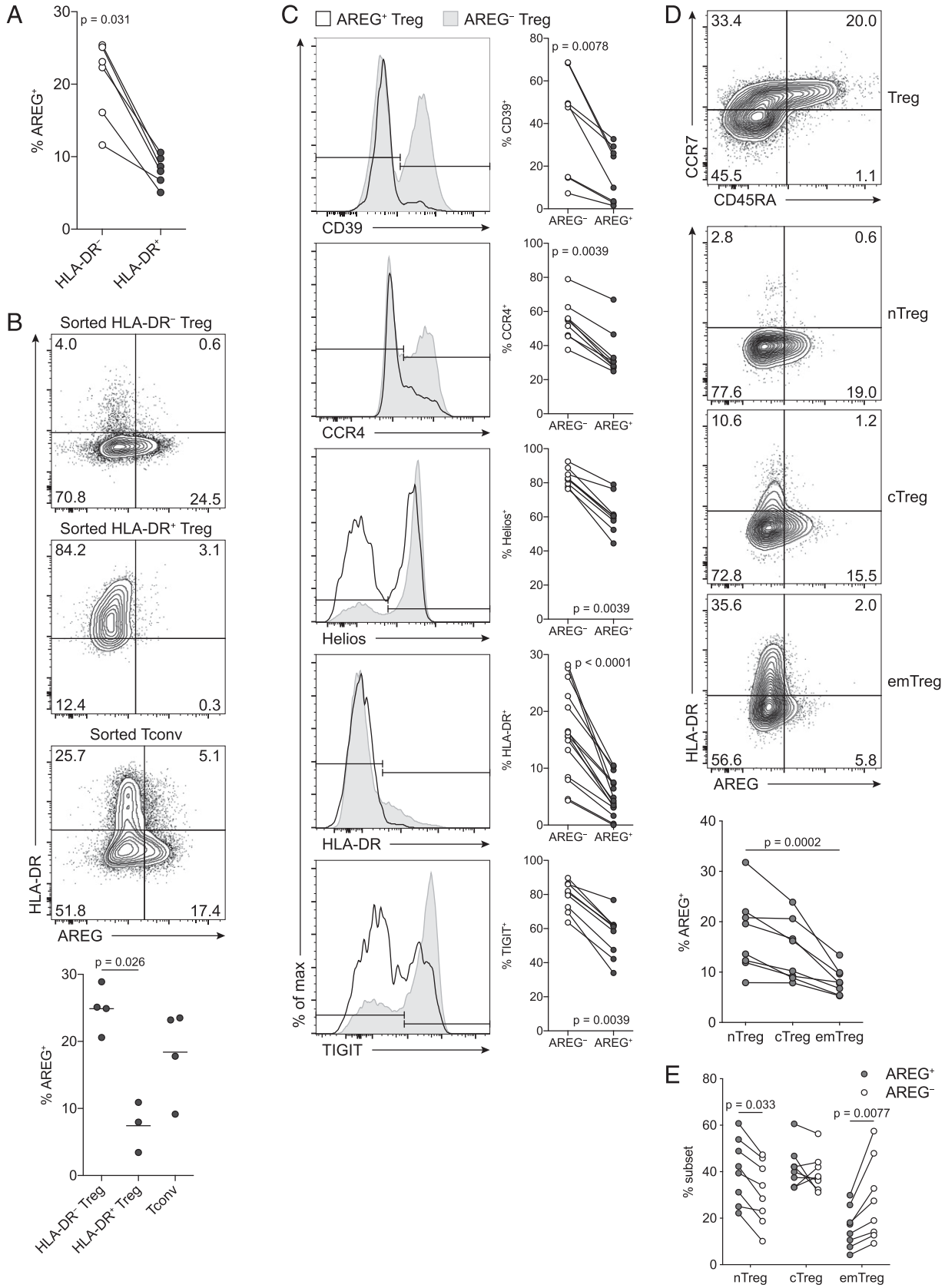

FIGURE 2. Human blood AREG-producing Tregs are enriched for a noneffector phenotype. (**A**) Flow-sorted Tregs ($CD4^+CD25^{hi}CD127^{lo}$) were activated with IL-2 (100 IU/ml) and 1:1 anti-CD3/CD28–coated beads for 4 d and then restimulated with PMA, ionomycin, and brefeldin A (4 h). AREG expression was measured on gated HLA-DR^+ and HLA-DR^- Tregs ($n = 6$). (**B**) AREG expression in flow-sorted HLA-DR^+ and HLA-DR^- Tregs (both $CD4^+CD25^{hi}CD127^{lo}$) or total Tconvs ($CD4^+CD25^{lo}CD127^{hi}$) activated as in (A) for 5 d and restimulated with PMA, ionomycin, and brefeldin A (4 h) (top, representative; bottom, $n = 3$–4). (**C**–**E**) CD4-enriched PBMCs were activated with PMA, ionomycin, and brefeldin A (4 h), and Tregs were gated as $CD4^+CD25^{hi}FOXP3^+$. (C) Representative (left) and quantified (right) expression of CD39 ($n = 8$), CCR4 ($n = 9$), Helios ($n = 9$), HLA-DR ($n = 15$), and TIGIT ($n = 9$) within $AREG^+$ and $AREG^-$ Tregs. (D) Treg expression of AREG within naive (nTreg; $CD45RA^+CCR7^+$), central memory *(Figure legend continues)*

TCR activation, but not IL-18 or IL-33, increases AREG expression in human blood Tregs

Next, we investigated what factors might promote AREG expression in human Tregs. TCR stimulation is dispensable for AREG expression by mouse Tregs in vitro and in vivo (9) but induces its production in human $CD4^+$ T cells (20). Sorted blood Tregs ($CD4^+CD25^{hi}CD127^{lo}$) and Tconvs ($CD4^+CD25^{lo}CD127^{hi}$) activated via the TCR transiently upregulated expression of *AREG* mRNA after 30 min, but levels quickly declined thereafter (Fig. 3A). Nevertheless, at the protein level, both TCR-activated Tregs and Tconvs had increased proportions of $AREG^+$ cells compared with their 4-d unstimulated counterparts (Fig. 3B), and there was a trend, although NS, to higher secretion of AREG in TCR-activated cells (Fig. 3C). Notably, as with ex vivo cells, in all cases the amount/proportion of AREG production by Tregs was lower than that of Tconvs (Fig. 3A–C). Thus, although TCR stimulation can induce AREG production by human blood Tregs, its expression is not a distinctive feature compared with other $CD4^+$ T cells.

Tissue damage is thought to lead to the release of alarmins that drive AREG expression in immune cells. For example, in mice, lung- and gut-resident ILC2s produce AREG in response to IL-33 (30, 31), and a subset of splenic Tregs secrete AREG in vitro upon exposure to IL-18 or IL-33 (9). We therefore hypothesized that epithelial cell–derived tissue damage signals such as IL-18 or IL-33 might drive AREG production in human Tregs. Human blood Tregs and Tconvs were activated through their TCR in the presence or absence of IL-18 and/or IL-33. We found that neither IL-18 nor IL-33 significantly modulated *AREG* mRNA expression over time (Fig. 3D) or AREG protein expression in Tregs or Tconvs after 4 d (Fig. 3E).

The lack of an effect of IL-18 or IL-33 on AREG may be related to the absence of the respective receptor on $CD4^+$ T cells in blood. We thus examined expression of IL-18R and ST2 (IL-33Rα) on ex vivo Tregs and Tconvs. We found that a subset of memory ($CD45RA^-$) Tregs and Tconvs expressed IL-18Rα ex vivo (Fig. 3F); thus, the lack of an IL-18–mediated effect is likely unrelated to IL-18R expression. In contrast, we were unable to detect ST2 expression on human blood Tregs or Tconvs using a commercial Ab (Fig. 3G).

Human Tregs from blood, tonsils, synovial fluid, colon, and lung tissue do not express ST2

To account for the possible low sensitivity of commercially available anti-human ST2 mAbs, we used phage display to generate a series of synthetic anti-human ST2 mAbs. The IL-33R is a heterodimer of ST2 and the accessory protein IL-1RAP, which complexes upon IL-33 binding (32). Candidate mAbs were first evaluated with an ST2- or IL-1RAP–transfected cell line (Supplemental Fig. 1A) and ST2-transduced human T cells (Supplemental Fig. 1B), with several clones exhibiting high specificity and sensitivity compared with commercial options. To validate specificity on endogenous ST2-expressing cells, we stained human blood ILC2s (gated as $Lin^-CD127^+CD161^+CRTH2^+$) after 24 h culture with IL-2 and IL-33 (33), revealing ST2 expression on a subset of cultured ILC2s (Supplemental Fig. 1C). Expression of ST2 was also consistently detected on $CD19^+$ B cells (Supplemental Fig. 1D). However, even with these high-affinity synthetic mAbs, we were unable to detect ST2 on blood Tregs or Tconvs ex vivo (Fig. 4A), explaining the lack of an IL-33–mediated effect on AREG expression (Fig. 3).

We next hypothesized that ST2 expression may be induced on human blood Tregs after coculture with $ST2^+$ APCs and IL-33 (15, 34). Sorted blood Tregs were cocultured with immature or cytokine-matured moDCs for 13 d, with IL-2 and IL-33 supplemented every 2–3 d. Although immature moDCs expressed ST2, which was downregulated upon cytokine-induced maturation (Fig. 4B), ST2 expression was not found on cocultured Tregs, with or without IL-33 (Fig. 4C).

Mouse $ST2^+$ Tregs primarily reside in nonlymphoid tissues such as the colon, visceral adipose tissue, and liver (12, 35–37), so we speculated that human $ST2^+$ Tregs may also be tissue-restricted. We obtained samples of human tissues—tonsil, synovial fluid, colonic lamina propria, bronchoalveolar lavage, and lung tissue—and used flow cytometry to seek $ST2^+$ Tregs. All tissues were considered normal (i.e., from healthy individuals or from noncancerous biopsy specimens in patients) except for synovial fluid and bronchoalveolar lavage, which were from patients with juvenile idiopathic arthritis and patients post–lung transplantation, respectively. ST2 detection was unaffected by collagenase digestion (Supplemental Fig. 1E), permitting us to evaluate ST2 expression on Tregs from tissues isolated with collagenase. As blood ILC2s upregulated ST2 after short-term culture with IL-2 and IL-33 (Supplemental Fig. 1C), we incubated blood and tissue samples for 24 h in the presence of IL-2 and IL-33. ST2 expression was found on a subset of $CD19^+$ B cells in blood ($1.6 \pm 0.6\%$ ex vivo, $1.1 \pm 0.4\%$ after 24 h culture with IL-2 and IL-33; mean ± SD, $n = 7–8$) and tonsils ($0.8 \pm 0.5\%$ ex vivo, $0.6 \pm 0.4\%$ after 24 h culture with IL-2 and IL-33; mean ± SD, $n = 5$) (Fig. 4D). However, ST2-expressing $FOXP3^+$ Tregs were not consistently detected in these tissues (Fig. 4D).

Human ST2-transduced Tregs exhibit enhanced proliferation and maintain their T cell suppressive capacity in response to IL-33

Because of extensive data in mice supporting the concept that $ST2^+$ Tregs might have desirable therapeutic properties, including tissue repair function, high suppressive capacity, and enhanced stability, we next engineered human $ST2^+$ Tregs to examine their potential as a cell therapy. Sorted naive Tregs ($CD4^+CD25^{hi}CD127^{lo}CD45RA^+$) were transduced with a bidirectional-promoter lentiviral vector encoding ST2 and truncated NGFR (transduction marker) or a control vector encoding NGFR only. Cells were expanded for 2 wk with artificial APCs and high-dose IL-2; transduced cells were bead-purified by NGFR selection after the first 7 d. As expected, ST2–NGFR–transduced Tregs (ST2 Tregs) expressed high levels of ST2 compared with their NGFR-transduced Treg (NGFR Treg) counterparts (Supplemental Fig. 2A). Consistent with endogenous mouse $ST2^+$ Tregs (17), human ST2 Tregs responded to IL-33 via phosphorylation of p38 MAPK and the p65 subunit of NF-κB (Supplemental Fig. 2B), confirming expression of a fully functional IL-33R heterodimer.

(cTreg; $CD45RA^-CCR7^+$), and effector memory Treg (emTreg; $CD45RA^-CCR7^-$) subsets ($n = 8$). Representative subset gates within Tregs (top), representative AREG expression (middle), and quantification (bottom). (E) Tregs were gated as $AREG^+$ or $AREG^-$ and then quantified as nTreg, cTreg, or emTreg as in (D) ($n = 8$). Dots in (A)–(E) represent independent donors; bars in (B) and (E) represent means. Significance was determined by Wilcoxon matched-pairs signed-rank test for (A) and (C), Kruskal–Wallis test with Dunn multiple comparisons test for (B), Friedman test with Dunn multiple comparisons test for (D), and matched two-way ANOVA with Sidak test for (E).

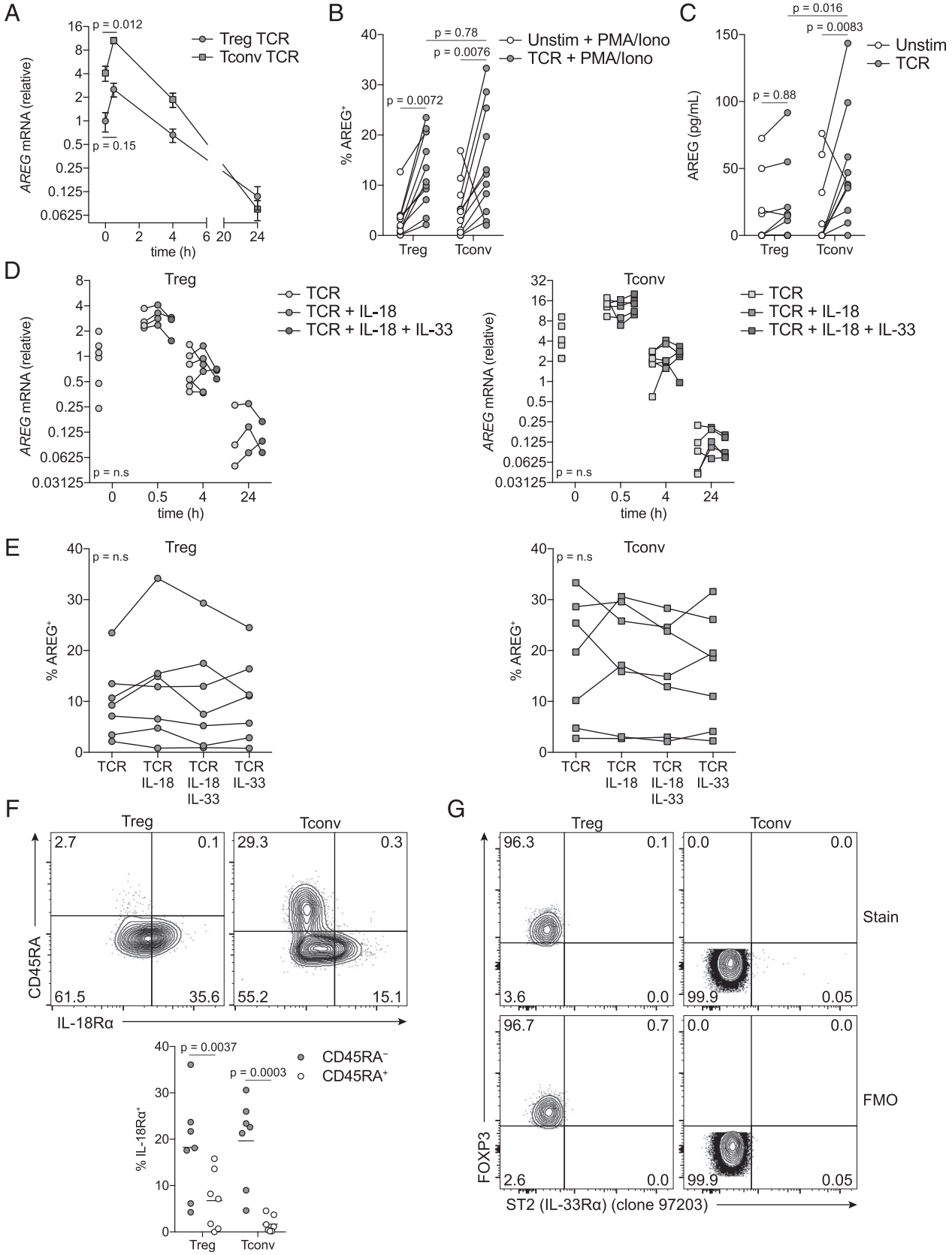

FIGURE 3. TCR activation, but not IL-18 or IL-33, increases AREG expression in human blood Tregs. (**A**–**E**) Flow-sorted Tregs ($CD4^+CD25^{hi}CD127^{lo}$) and Tconvs ($CD4^+CD25^{lo}CD127^{hi}$) were activated with IL-2 (100 IU/ml) and 1:1 anti-CD3/CD28–coated beads in the presence or absence of IL-18 and/or IL-33 (20 ng/ml each). (A) *AREG* mRNA expression at the indicated times was determined by quantitative PCR and normalized to *RPL13A* and *SDHA* (n = 4–7 per timepoint); data are plotted on a $\log_2$ axis. (B–C) Cells were activated for 4 d. (B) AREG protein expression was quantified by flow cytometry in cells restimulated with PMA, ionomycin, and brefeldin A (4 h; n = 11), and (C) secreted AREG was measured in supernatants collected before restimulation (n = 8). (D) *AREG* mRNA expression was determined as in (A) (n = 3–6 per timepoint); data are plotted on a $\log_2$ axis. (E) AREG protein expression was quantified as in (C) (n = 7). (**F** and **G**) Ex vivo Treg ($CD4^+CD25^{hi}FOXP3^+$) and Tconv ($CD4^+CD25^{lo}FOXP3^-$) expression *(Figure legend continues)*

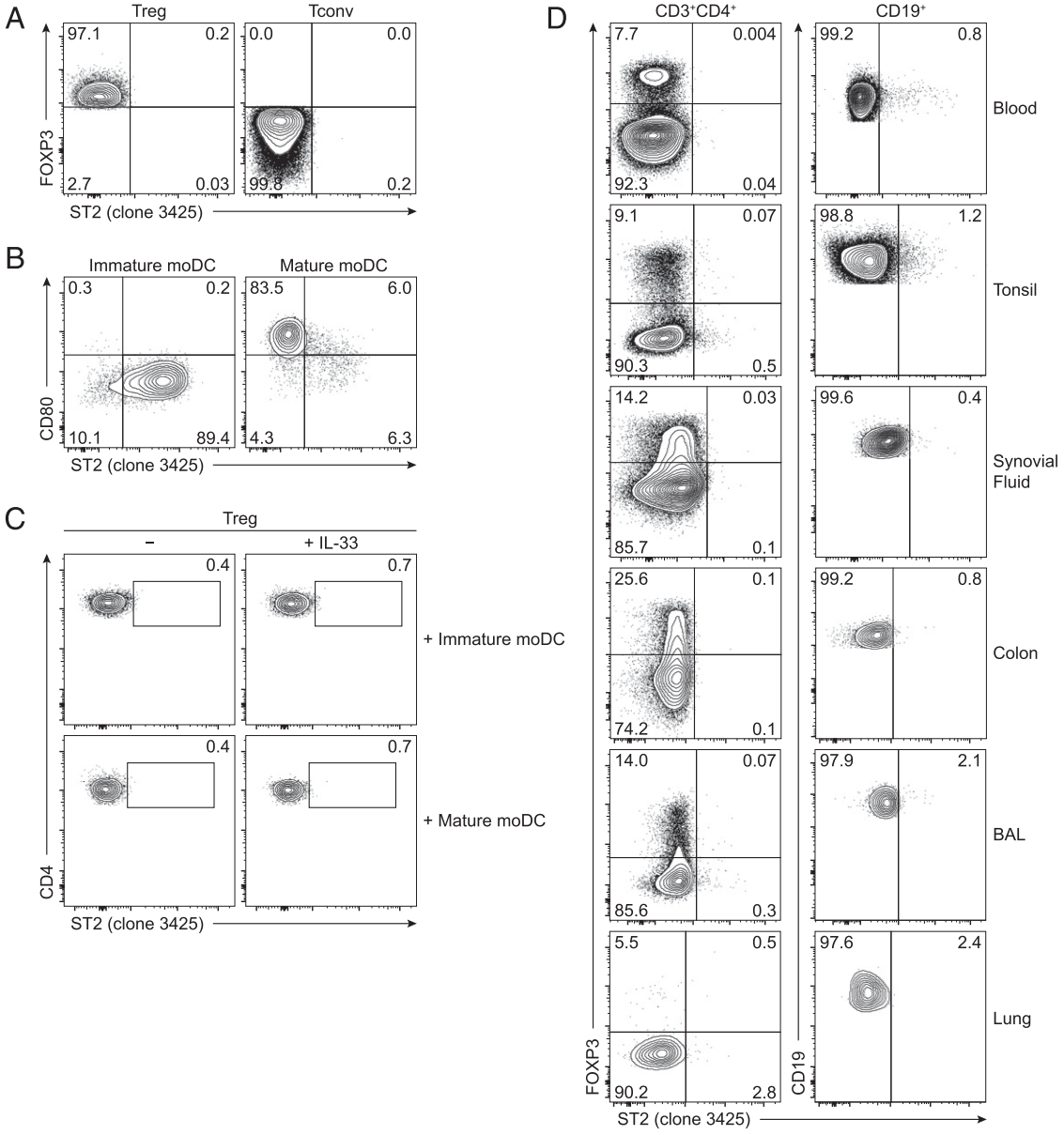

FIGURE 4. Human Tregs from blood, tonsils, synovial fluid, colon, and lung tissue do not express ST2. ST2 expression was evaluated with a synthetic anti-human ST2 (clone 3425) mAb. (**A**) Representative ex vivo ST2 expression on Tregs ($CD4^+CD25^{hi}FOXP3^+$) and Tconvs ($CD4^+CD25^{lo}FOXP3^-$) from CD4-enriched PBMCs (n = 3). (**B** and **C**) Immature or cytokine-matured moDCs were irradiated and cocultured 1:1 with flow-sorted Tregs ($CD4^+CD25^{hi}CD127^{lo}$) and IL-2 (1000 IU/ml) for 12 d in the presence or absence of IL-33 (20 ng/ml) added every 2–3 d. (B) Representative ST2 expression on immature and cytokine-matured moDCs before coculture (n = 6). (C) Representative ST2 expression on Tregs after coculture with immature or cytokine-matured moDCs in the presence or absence of IL-33 (n = 4 independent Treg donors). (**D**) Mononuclear cells from blood (n = 8), tonsil (n = 5), synovial fluid (n = 3), colon (n = 2), bronchoalveolar lavage (BAL; n = 3), and lung tissue (n = 2) were cultured with IL-2 (100 IU/ml) and IL-33 (50 ng/ml) for 24 h. Representative ST2 expression on $CD3^+CD4^+CD8^-CD56^-$ T cells or $CD19^+$ B cells for the indicated tissues.

As IL-33 expands mouse $ST2^+$ Tregs in vitro and in vivo (12, 15, 36), we asked whether IL-33 affects ST2 Treg proliferation. NGFR or ST2 Tregs were labeled with CPD and then TCR-activated with IL-2 in the presence or absence of IL-33 for 4 d. ST2 Tregs exhibited enhanced TCR-dependent proliferation with IL-33. In contrast, IL-33 alone (with IL-2) did not significantly affect Treg proliferation (Fig. 5A). Similarly, when IL-33 was added during Treg expansion, we found enhanced expansion with unchanged cell viability and increased expression of Ki-67 (Supplemental Fig. 3A–C). These data demonstrate that IL-33 can enhance ST2 Treg proliferation and expansion in a TCR-dependent manner.

We next assessed the effects of IL-33 on the TCR-dependent immunosuppressive function of ST2 Tregs. ST2 Tregs expanded

of (F) IL-18Rα (n = 7) and (G) ST2 (clone 97203; n = 5) expression from CD4-enriched PBMCs. (A) depicts mean ± SEM; dots in (B)–(F) represent independent donors. Significance was determined by two-way ANOVA with Dunnett test for (A), matched two-way ANOVA with Tukey test for (B) and (C), matched two-way ANOVA with Dunnett test for (D) and (E), and matched two-way ANOVA with Sidak test for (F). FMO, fluorescence minus one; n.s., not significant.

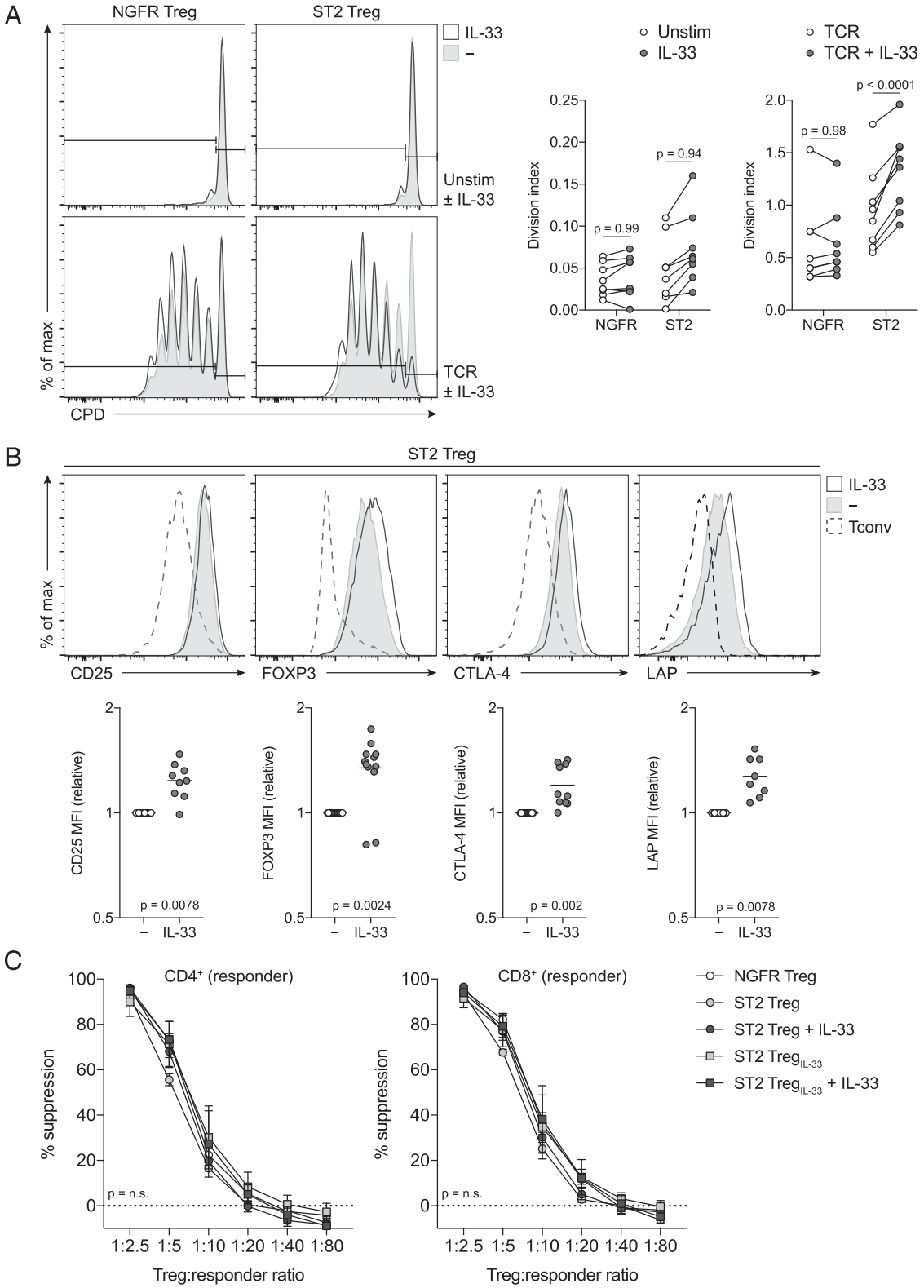

FIGURE 5. Human ST2-transduced Tregs exhibit enhanced proliferation and maintain their T cell suppressive capacity in response to IL-33. (**A**) Expanded NGFR- or ST2-transduced naive Tregs (flow-sorted as $CD4^+CD25^{hi}CD127^{lo}CD45RA^+$) were labeled with CPD and activated with IL-2 (100 IU/ml) in the presence or absence of 1:1 anti-CD3/CD28–coated beads and IL-33 (20 ng/ml) for 4 d. Representative CPD dilution (left) and division index (right, $n = 9$). (**B**) Expression of CD25 ($n = 7$), FOXP3 ($n = 15$), CTLA-4 ($n = 13$), and LAP ($n = 8$) on ST2-transduced naive Tregs expanded for 12 d with or without IL-33 (20 ng/ml) added on days 7, 9, and 11 (top, representative; bottom, quantification); relative MFI data are plotted on a $\log_2$ axis. Expression by expanded naive Tconvs (flow-sorted as $CD4^+CD25^{lo}CD127^{hi}CD45RA^+$) is shown for reference. (**C**) Expanded NGFR- or ST2-transduced naive Tregs [expanded with or without IL-33 as in (B)] and allogeneic $CD3^+$ T cells (responder cells) were differentially labeled with CPD, cocultured at the indicated ratios, and activated with anti-CD3/CD28–coated beads (1:16 beads/responder cells) and IL-33 (20 ng/ml) for 4 d ($n = 4$ independent Treg donors). Suppression of proliferation within $CD4^+$ (left) and $CD8^+$ (right) T cells. Dots in (A) and (B) represent individual donors; bars in (B) represent means. (C) depicts mean ± SEM. Significance was determined by matched two-way ANOVA with Tukey multiple comparisons test for (A), Wilcoxon matched-pairs signed-rank test for (B), and Friedman test with Dunn multiple comparisons test of the total areas under each curve for (C). MFI, geometric mean fluorescence intensity; n.s., not significant.

in the presence of IL-33 had significantly increased expression of the Treg-associated proteins CD25, FOXP3, CTLA-4, and LAP (Fig. 5B) and maintained high Helios expression (Supplemental Fig. 3D). IL-33 also potentiated TCR activation in ST2 Tregs, as seen by elevated expression of CD39, CD71, and HLA-DR (Supplemental Fig. 3E). We found no change in GATA3 expression in response to IL-33 (Supplemental Fig. 3E).

To measure the suppressive capacity of ST2 Tregs in response to IL-33, NGFR or ST2 Tregs (some expanded with IL-33) were cocultured with allogeneic $CD3^+$ T cell responders and TCR-activated for 4 d in the presence or absence of IL-33. In all cases, Tregs were equally able to suppress $CD4^+$ and $CD8^+$ T cell proliferation. IL-33 did not affect the ST2 Treg suppressive function, either when added during expansion or during Treg:responder coculture (Fig. 5C).

IL-33 alters the transcriptomic and cytokine profile of human ST2-transduced Tregs

To further characterize IL-33–dependent changes in ST2 Tregs, we conducted transcriptome profiling of cells activated with IL-2 and TCR with or without IL-33. Short-term culture with IL-33 induced gene expression associated with negative regulation of NF-κB and p38 signaling (*NFKBIZ* and *DUSP8*; Fig. 6A). IL-33 also upregulated expression of *IL13*, a known IL-33–upregulated gene in mouse Th2 cells (14), and the Th2- and Treg-homing chemokine *CCL22* (Fig. 6A). Transcript-level expression of *KLF2*, which controls Treg homing to lymphoid organs, markedly decreased with IL-33 treatment (Fig. 6A).

We used gene set enrichment analysis to identify coordinated changes in gene expression. We found strong enrichment in genes involved in cell cycle progression as well as genes downstream of E2F transcription factors upon IL-33 treatment of ST2 Tregs (Fig. 6B). IL-33–treated ST2 Tregs also showed strong enrichment for Myc targets and mTORC1 signaling (Fig. 6B). Thus, short-term exposure to IL-33 promotes ST2 Treg proliferation and leads to changes in pathways associated with metabolism.

To examine cytokine production by ST2 Tregs, NGFR or ST2 Tregs were TCR-activated for 4 d with or without IL-33. In comparison with NGFR Tregs, IL-33 resulted in increased ST2 Treg secretion of the myeloid-regulating cytokines GM-CSF and IL-13 (Fig. 6C), as well as the T cell– and myeloid-attracting chemokines IL-8, CCL3, and CCL5 (Fig. 6D). In contrast, no difference in IL-10 production, a characteristic cytokine of mouse $ST2^+$ Tregs (35), was found (Fig. 6E). No differences were observed in CCL4, IFN-γ, IL-4, IL-17A, IL-22, and TNF-α (data not shown). Collectively, IL-33, by promoting lymphoid-tissue exit, elevated cytokine production, and potential metabolic reprogramming, may poise ST2 Tregs to adopt an effector-like phenotype in peripheral tissues.

IL-33 innately upregulates AREG expression in human ST2-transduced Tregs

Given the link between IL-33 signaling and AREG expression in mouse Tregs, we asked whether human ST2 Tregs had greater tissue repair potential via AREG expression. NGFR or ST2 Tregs were activated for 4 d with IL-2 in the presence or absence of TCR stimulation and IL-33, followed by restimulation with PMA and ionomycin. Whereas TCR-activated Tregs exhibited no change in AREG expression with IL-33, ST2 Tregs cultured with IL-33 alone (with IL-2) had significantly elevated AREG expression (Fig. 7A). Moreover, analysis of AREG expression by TCR-activated cells within each CPD fraction revealed that AREG expression was progressively lost with each subsequent cell division in both NGFR and ST2 Tregs (Fig. 7B), consistent with data from ex vivo Tregs (Fig. 2D). Thus, IL-33 innately upregulates AREG in a TCR-independent fashion on human ST2 Tregs.

Human ST2-transduced Tregs induce alternatively activated monocytes

Monocytes/macrophages are central orchestrators of the tissue repair process (38). Human Tregs can induce the alternative activation of monocytes through contact-dependent mechanisms and soluble factors, including IL-4, IL-10, and IL-13 (39, 40). To test the possibility that IL-33 may affect Treg-mediated regulation of monocytes, NGFR or ST2 Tregs were cocultured with allogeneic $CD14^+$ monocytes for 40 h. Tregs downregulated the Ag presentation–related molecules CD86 and HLA-DR on monocytes in a Treg:monocyte ratio–dependent manner (Fig. 8A). Notably, ST2 Tregs were better able to augment monocyte expression of the M2-associated protein CD163 (scavenger receptor), and there was a trend, although not significant, to CD206 upregulation (mannose receptor) compared with NGFR Tregs, particularly at higher Treg:monocyte ratios (Fig. 8B). These changes in monocyte phenotype were largely independent of the addition of rIL-33 (Fig. 8A, 8B), suggesting that endogenous IL-33 contributes to a juxtacrine Treg–monocyte cross-talk mechanism. Indeed, IL-33 expression has been detected in human monocytes at the RNA and protein level but not found to be secreted (41).

Discussion

Tregs with tissue repair function would be attractive for a variety of therapeutic applications. To our knowledge, we are the first to identify and characterize AREG-producing Tregs in human blood and multiple tissue types, noting significant divergences from mouse Tregs. Specifically, human AREG-producing Tregs are present at lower frequencies than Tconvs, exhibit a noneffector phenotype, and, at least for the tissues we examined, are not selectively upregulated in tissues compared with blood. Naturally occurring human $ST2^+$ Tregs were not found in blood, tonsil, synovial fluid, colon, or lung tissue. Engineered ST2 Tregs, however, exhibited IL-33–driven AREG expression and an enhanced ability to polarize monocytes toward an M2-like phenotype, suggesting that engineered human Tregs may promote tissue repair, although the specific settings in which these cells could be applied to take advantage of this function require more investigation.

AREG production by mouse Tregs has emerged as an important element of TCR-independent tissue-protective function (5, 9, 42). Accordingly, AREG mRNA and protein expression is highly enriched in mouse Tregs compared with Tconvs, particularly in Tregs resident in nonlymphoid tissues (5, 9, 11, 12, 42). In contrast, although human Tregs produced AREG, the levels were consistently lower than their Tconv counterparts; this finding held true for cells isolated from blood and multiple tissue types, including tonsil, synovial fluid, colon, and lung. Blood Treg AREG expression could not be enhanced by IL-18 or IL-33 stimulation, in contrast to mouse Tregs (9). In mouse influenza infection, AREG production by lung Tregs was critical for tissue protection (9), but in other settings, AREG production by multiple cell types is necessary to promote epithelial cell growth (43). Thus, our data suggest that human Tregs have the capacity to contribute to AREG-mediated tissue repair, but because this is not a defining characteristic of these cells, they likely function in concert with other AREG-producing cells.

Contrary to our expectations, we could not identify human $ST2^+$ Tregs in blood, in a variety of tissue types (tonsil, synovial fluid, colon, and lung), or after coculture with IL-33–treated $ST2^+$ APCs. We also failed to detect $ST2^+$ Tregs in human omental adipose tissue from lean or obese subjects (44). These data

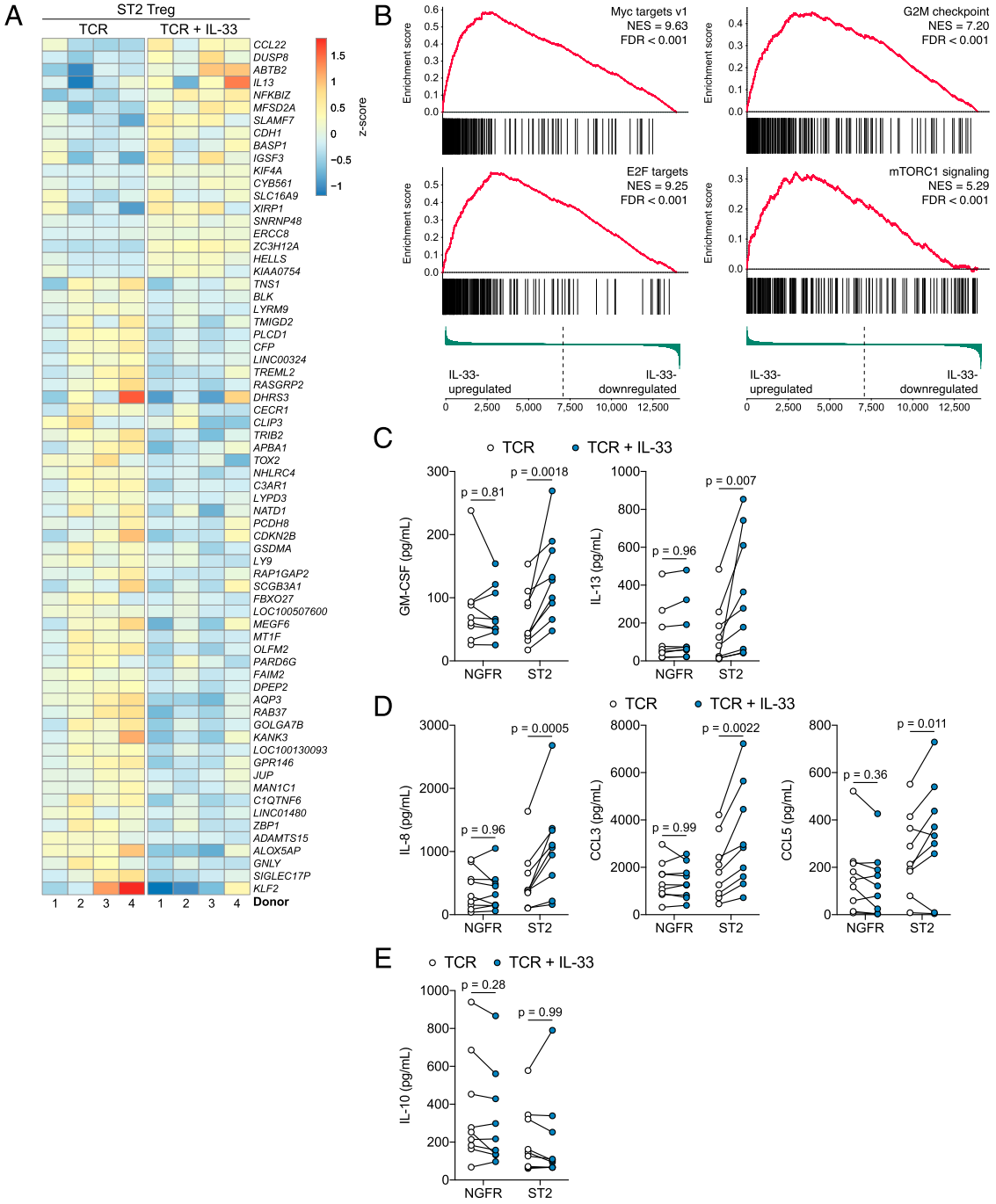

FIGURE 6. IL-33 alters the transcriptomic and cytokine profile of human ST2-transduced Tregs. (**A** and **B**) RNA sequencing was performed on expanded ST2-transduced naive Tregs activated with IL-2 (100 IU/ml) and 1:1 anti-CD3/CD28–coated beads with or without IL-33 (20 ng/ml) for 16 h ($n = 4$). (A) Heat map of differentially expressed genes (selected by Benjamini–Hochberg–corrected $p < 0.05$ and $\log_2$[fold change] > 1); columns represent matched donors (indicated at bottom). Color scale represents the per-gene z-score. (B) Gene set enrichment plots for selected Hallmark gene sets in IL-33–upregulated genes, with normalized enrichment scores (NES) and Benjamini–Hochberg–corrected false discovery rate (FDR). (**C**–**E**) Expanded NGFR- or ST2-transduced naive Tregs were activated as in (A) and (B) for 4 d. Cytokine and chemokine concentrations in supernatants were measured by cytometric bead array ($n = 9$). Significance for (C)–(E) was determined by matched two-way ANOVA with Sidak multiple comparisons test.

contrast with accumulating evidence for the biological importance of mouse ST2$^+$ Tregs in a multitude of tissue types, including blood (45), lymphoid tissues (15, 17, 46), visceral adipose tissue (35, 36, 47), colon (12), lung (9, 48), liver (37), and skeletal muscle (5, 10). However, in line with a previous study (33), we detected ST2 expression on human blood ILC2s, as well as on blood and tonsillar CD19$^+$ B cells and immature moDCs. Whether other pathways beyond the IL-33/ST2 axis govern human Treg maintenance and reparative function in tissues requires further study.

Because we could not find endogenous human ST2-expressing Tregs, we engineered an artificial source of ST2$^+$ Tregs to examine their potential as a cell therapy. Interestingly, overexpression of ST2 in human blood Tregs recapitulated some of the IL-33–dependent effects seen in mice (15, 45), including canonical IL-33 signal transduction as well as increased TCR-dependent expansion and activation. Of note, ST2 Treg production of AREG could be augmented innately by IL-33 in a TCR-independent manner. In addition, using transcriptome analysis, we found that

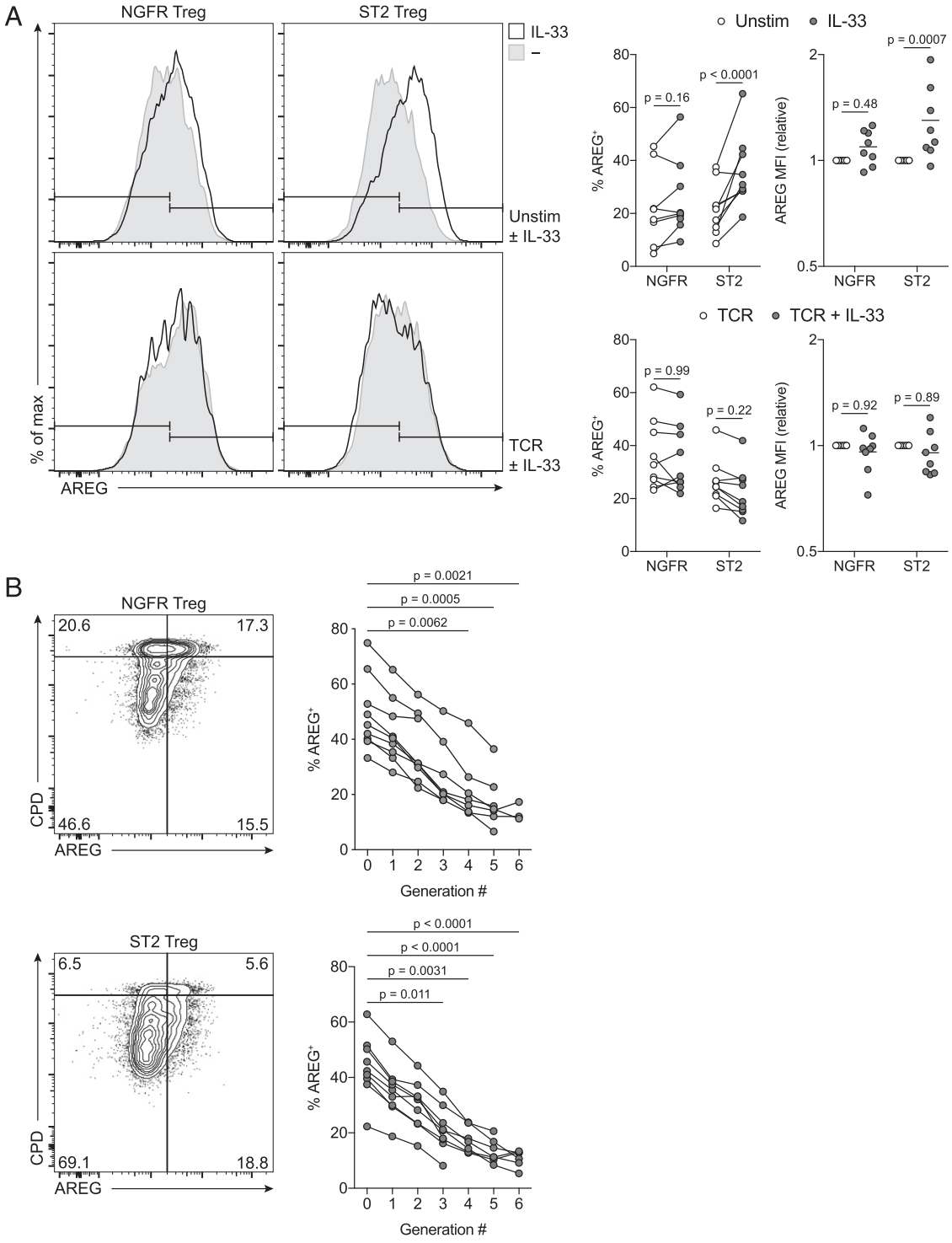

FIGURE 7. IL-33 innately upregulates AREG expression in human ST2-transduced Tregs. Expanded NGFR- or ST2-transduced naive Tregs were labeled with CPD and activated with IL-2 (100 IU/ml) in the presence or absence of 1:1 anti-CD3/CD28–coated beads and IL-33 (20 ng/ml) for 4 d and then restimulated with PMA, ionomycin, and brefeldin A (4 h; $n = 9$). (**A**) Representative (left) and quantified (right) intracellular AREG expression; MFI was normalized per cell type in each graph. (**B**) AREG expression (left) was quantified within each CPD fraction (right; Generation #) from NGFR Tregs (top) or ST2 Tregs (bottom) activated with IL-2 and 1:1 anti-CD3/CD28–coated beads for 4 d and restimulated as in (A). Dots represent individual donors. Significance was determined by matched two-way ANOVA with Tukey multiple comparisons test for (A) and Kruskal–Wallis test with Dunn multiple comparisons test for (B). MFI, geometric mean fluorescence intensity.

IL-33 induced the Myc and mTORC1 pathways and downregulated the lymphoid-retention gene *KLF2*, suggesting that IL-33 may direct ST2 Tregs to home to nonlymphoid tissues. These data suggest that cell therapy with ST2 Tregs may enable preferential migration to nonlymphoid tissues, where they could have an innate-like tissue-protective function.

The tissue repair capacity of human Tregs may be an innate function that operates independently from their classical TCR-dependent suppressive function. TCR-induced proliferation and differentiation coincided with a progressive loss of AREG, and AREG$^+$ Tregs expressed a lower proportion of many Treg activation/effector proteins (CD39, CCR4, HLA-DR, and TIGIT).

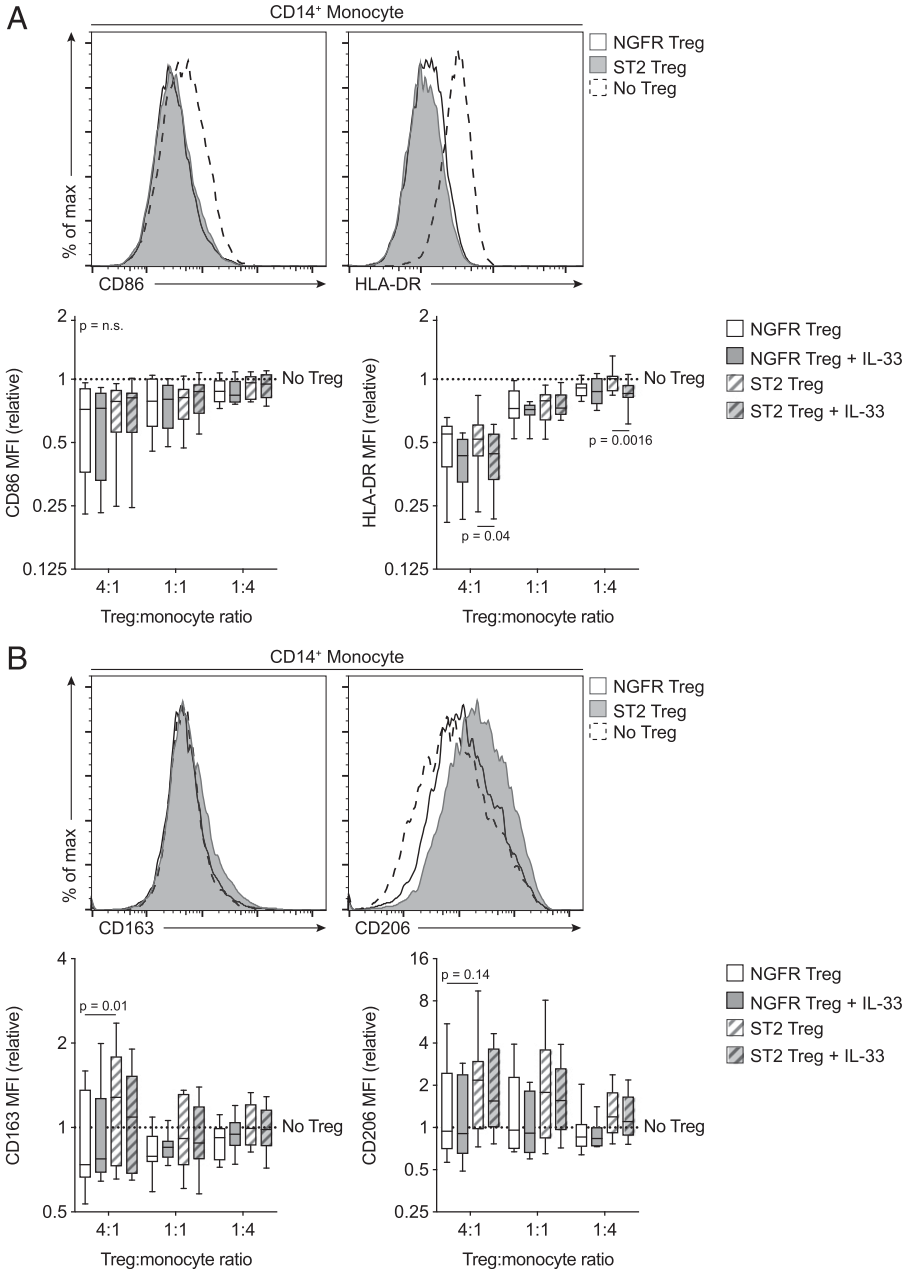

FIGURE 8. Human ST2-transduced Tregs drive alternative activation in monocytes. Expanded NGFR- or ST2-transduced naive Tregs and allogeneic $CD14^+$ monocytes were cocultured at the indicated ratios and activated with IL-2 (100 IU/ml), OKT3 (1 μg/ml), and IL-33 (20 ng/ml) for 40 h (n = 8–12 Treg–monocyte pairs). Representative (top, showing 4:1 Treg/monocyte cocultures activated with IL-2 and OKT3) and box-and-whisker plots (bottom) of $CD14^+$ monocyte expression of (**A**) CD86 and HLA-DR and (**B**) CD163 and CD206. MFI was normalized per $CD14^+$ monocyte donor activated with IL-2 and OKT3 (±IL-33); relative MFI data are plotted on a $\log_2$ axis. Dotted line (no Treg) represents $CD14^+$ monocytes alone activated with IL-2 and OKT3 (±IL-33). In (A) and (B), boxes span the interquartile range, center lines represent the median, and whiskers cover the minimum and maximum. Significance in (A) and (B) was determined by two-way ANOVA with Dunnett multiple comparisons test. MFI, geometric mean fluorescence intensity; n.s., not significant.

Moreover, ST2-transduced Tregs upregulated AREG innately in response to IL-33, mirroring our observations in endogenous Tregs and suggesting that regulation of AREG expression is TCR-independent.

Human ST2-transduced Tregs also exhibited elevated tissue repair potential by modulation of other cell types. Beyond AREG, which may drive the repair process by directly acting on parenchymal cells, we found that human ST2 Tregs secreted more of the myeloid-targeting cytokines and chemokines GM-CSF, IL-13, IL-8, CCL3, and CCL5. This finding prompted us to investigate their capacity to modulate monocytes/macrophages, which are considered to be key orchestrators of tissue repair. ST2 Tregs induced a shift in monocytes toward an alternatively activated phenotype to a greater extent than control Tregs, characterized by upregulated expression of CD163 and a trend toward higher CD206. These ST2 Treg–primed, alternatively activated monocytes/macrophages may be better poised to mediate tissue repair.

Nevertheless, ST2 transduction alone in human Tregs does not completely confer the IL-33–dependent, tissue-specific phenotype seen in mouse Tregs. IL-33 was initially identified as a Th2-associated cytokine (49), and $ST2^+$ Tregs have been reported to be Th2-biased (45, 48); we found an IL-33–dependent increase in IL-13 but unchanged IL-10 and GATA3. Furthermore, the addition of IL-33 in vitro, either during ST2 Treg expansion or during T cell coculture, had no effect on their suppressive capacity. These data suggest that, in human ST2 Tregs, IL-33 may mediate an incomplete polarization toward a Th2-like phenotype. This finding is in line with data from mouse studies, which found that, although isolated $ST2^+$ Tregs were inherently more suppressive in vitro than their $ST2^-$ Treg counterparts, the addition of IL-33 had no beneficial effect (15, 45). Taken together, IL-33 does not appear to be the central factor driving the unique phenotype and functions of tissue $ST2^+$ Tregs seen in mice: ST2 may instead simply be a marker of a specific subset of tissue-localized Tregs. Recent evidence that mouse $ST2^+$ Tregs arise in normal numbers and frequencies despite the absence of IL-33 signals (45) supports this notion.

Our work has several limitations. Notably, most blood and tissue samples were from healthy individuals or from noncancerous areas;

only synovial fluid and bronchoalveolar lavage samples were from patients with juvenile idiopathic arthritis and patients post–lung transplantation, respectively. Because IL-33 is elevated in the airways during asthma exacerbations (50) and in the inflamed mucosa of patients with ulcerative colitis (51–53), future investigations should assess ST2 expression in tissue Tregs from patients with active Th2-mediated diseases (54), as well as in muscle tissue (5, 36). Nevertheless, the absence of readily detectable human ST2$^+$ Tregs in human bronchoalveolar lavage and lung tissue suggests that ongoing clinical trials of anti–IL-33 and anti-ST2 Abs for asthma and atopic dermatitis (55–57) may not have the unintended effect of broad inhibition of Tregs.

Finally, although we show that human Tregs in multiple settings produce AREG, whether these cells use AREG to functionally drive tissue repair in a physiological context remains to be determined. A recent study suggests that a subset of human Tregs may be able to promote tissue repair via an AREG-independent mechanism (58). Future research with in vitro and in vivo models of wound healing will be required to better understand and harness the potential role of human Treg-mediated tissue repair in the context of cell therapy, via either AREG-dependent or AREG-independent mechanisms.

Treg cell therapy is rapidly emerging as a potential curative approach for a variety of immune-mediated conditions, including autoimmunity and graft-versus-host disease, where active tissue damage is an ongoing process. Although the observations that mouse Tregs can mediate tissue repair in multiple settings are an exciting prospect, our results with human Tregs reveal important differences from mouse models that should be taken into consideration in the clinical translation of therapeutic tissue-reparative Tregs.

Acknowledgments

We thank the donors and patients for participating in this study, netCAD at Canadian Blood Services for blood collection, the BC Children's Hospital BioBank for tonsil mononuclear cell samples, and Lori B. Tucker for assistance with synovial fluid sample collection. We thank Rebecca Mate, Rosa V. Garcia, and Dr. Sabine M. Ivison (University of British Columbia) for colon biopsy specimen procurement and assistance with sample processing. We thank Drs. Liran Levy and Tereza Martinu (University of Toronto) for assistance with identifying and processing the lung tissue samples. We thank the numerous research, clinical, and support staff who made collection of other tissue samples possible. We thank Dr. Guy Charron (Université de Montréal) for providing plasmids encoding ST2–GFP and IL-1RAP–GFP. We thank Dr. Lisa Xu for flow cytometry support, the University of British Columbia Antibody Lab (http://www.ablab.ca/) for Ab conjugation, and the University of British Columbia Biomedical Research Centre Sequencing Core for performing RNA sequencing. We thank Ryan Vander Werff and Dr. Romy E. Hoeppli (University of British Columbia) for advice regarding RNA sequencing data analysis.

iGenoMed Consortium Members

Alain Bitton and Rita Kohen (Department of Medicine, McGill University Health Centre, McGill University, Montreal, Quebec H4A 3J1, Canada)
Lawrence Joseph (Department of Epidemiology, Biostatistics and Occupational Health, McGill University Health Centre, McGill University, Montreal, Quebec H4A 3J1, Canada)
Gabrielle Boucher, Guy Charron, Anik Forest, Philippe Goyette, John D. Rioux, and Julie Thompson Legault (Department of Medicine, Montreal Heart Institute, University of Montreal, Montreal, Quebec H1T 1C8, Canada)
Christine Des Rosiers (Department of Nutrition, Montreal Heart Institute, University of Montreal, Montreal, Quebec H1T 1C8, Canada)
Jean Lachaine (Faculty of Pharmacy, University of Montreal, Montreal, Quebec H3T 1J4, Canada)
Sylvie Lesage (Department of Microbiology, Infectiology and Immunology, Maisonneuve-Rosemont Hospital, Université de Montréal, Montreal, Quebec H1T 2M4, Canada)
Brian White-Guay (Department of Family Medicine and Emergency Medicine, University of Montreal, Montreal, Quebec H3T 1J4, Canada)
Sabine Ivison and Megan K. Levings (Department of Surgery, BC Children's Hospital Research Institute, University of British Columbia, Vancouver, British Columbia V5Z 4H4, Canada)
Luc Vachon (Luc Vachon Consultant, Montreal, Quebec H2L 3V6, Canada)
Sophie Veilleux (Department of Management, Laval University, Québec, Quebec G1V 0A6, Canada)

Disclosures

The authors have no financial conflicts of interest.

References

1. Gliwiński, M., D. Iwaszkiewicz-Grześ, and P. Trzonkowski. 2017. Cell-based therapies with T regulatory cells. *BioDrugs* 31: 335–347.
2. Panduro, M., C. Benoist, and D. Mathis. 2016. Tissue Tregs. *Annu. Rev. Immunol.* 34: 609–633.
3. Lam, A. J., R. E. Hoeppli, and M. K. Levings. 2017. Harnessing advances in T regulatory cell biology for cellular therapy in transplantation. *Transplantation* 101: 2277–2287.
4. Zhang, C., L. Li, K. Feng, D. Fan, W. Xue, and J. Lu. 2017. 'Repair' Treg cells in tissue injury. *Cell. Physiol. Biochem.* 43: 2155–2169.
5. Burzyn, D., W. Kuswanto, D. Kolodin, J. L. Shadrach, M. Cerletti, Y. Jang, E. Sefik, T. G. Tan, A. J. Wagers, C. Benoist, and D. Mathis. 2013. A special population of regulatory T cells potentiates muscle repair. *Cell* 155: 1282–1295.
6. Villalta, S. A., W. Rosenthal, L. Martinez, A. Kaur, T. Sparwasser, J. G. Tidball, M. Margeta, M. J. Spencer, and J. A. Bluestone. 2014. Regulatory T cells suppress muscle inflammation and injury in muscular dystrophy. *Sci. Transl. Med.* 6: 258ra142.
7. Nosbaum, A., N. Prevel, H. A. Truong, P. Mehta, M. Ettinger, T. C. Scharschmidt, N. H. Ali, M. L. Pauli, A. K. Abbas, and M. D. Rosenblum. 2016. Cutting edge: regulatory T cells facilitate cutaneous wound healing. *J. Immunol.* 196: 2010–2014.
8. Panduro, M., C. Benoist, and D. Mathis. 2018. T_{reg} cells limit IFN-γ production to control macrophage accrual and phenotype during skeletal muscle regeneration. *Proc. Natl. Acad. Sci. USA* 115: E2585–E2593.
9. Arpaia, N., J. A. Green, B. Moltedo, A. Arvey, S. Hemmers, S. Yuan, P. M. Treuting, and A. Y. Rudensky. 2015. A distinct function of regulatory T cells in tissue protection. *Cell* 162: 1078–1089.
10. Kuswanto, W., D. Burzyn, M. Panduro, K. K. Wang, Y. C. Jang, A. J. Wagers, C. Benoist, and D. Mathis. 2016. Poor repair of skeletal muscle in aging mice reflects a defect in local, interleukin-33-dependent accumulation of regulatory T cells. *Immunity* 44: 355–367.
11. Cipolletta, D., M. Feuerer, A. Li, N. Kamei, J. Lee, S. E. Shoelson, C. Benoist, and D. Mathis. 2012. PPAR-γ is a major driver of the accumulation and phenotype of adipose tissue Treg cells. *Nature* 486: 549–553.
12. Schiering, C., T. Krausgruber, A. Chomka, A. Fröhlich, K. Adelmann, E. A. Wohlfert, J. Pott, T. Griseri, J. Bollrath, A. N. Hegazy, et al. 2014. The alarmin IL-33 promotes regulatory T-cell function in the intestine. *Nature* 513: 564–568.
13. Cipolletta, D., P. Cohen, B. M. Spiegelman, C. Benoist, and D. Mathis. 2015. Appearance and disappearance of the mRNA signature characteristic of Treg cells in visceral adipose tissue: age, diet, and PPARγ effects. *Proc. Natl. Acad. Sci. USA* 112: 482–487.
14. Guo, L., G. Wei, J. Zhu, W. Liao, W. J. Leonard, K. Zhao, and W. Paul. 2009. IL-1 family members and STAT activators induce cytokine production by Th2, Th17, and Th1 cells. *Proc. Natl. Acad. Sci. USA* 106: 13463–13468.
15. Matta, B. M., J. M. Lott, L. R. Mathews, Q. Liu, B. R. Rosborough, B. R. Blazar, and H. R. Turnquist. 2014. IL-33 is an unconventional alarmin that stimulates IL-2 secretion by dendritic cells to selectively expand IL-33R/ST2$^+$ regulatory T cells. *J. Immunol.* 193: 4010–4020.
16. Biton, J., S. Khaleghparast Athari, A. Thiolat, F. Santinon, D. Lemeiter, R. Herve, L. Delavallée, A. Levescot, S. Roga, P. Decker, et al. 2016. In vivo expansion of activated Foxp3$^+$ regulatory T cells and establishment of a type 2 immune response upon IL-33 treatment protect against experimental arthritis. *J. Immunol.* 197: 1708–1719.
17. Matta, B. M., D. K. Reichenbach, X. Zhang, L. Mathews, B. H. Koehn, G. K. Dwyer, J. M. Lott, F. M. Uhl, D. Pfeifer, C. J. Feser, et al. 2016. Peri-alloHCT IL-33 administration expands recipient T-regulatory cells that protect mice against acute GVHD. *Blood* 128: 427–439.
18. Becker, M., M. K. Levings, and C. Daniel. 2017. Adipose-tissue regulatory T cells: critical players in adipose-immune crosstalk. *Eur. J. Immunol.* 47: 1867–1874.
19. Zandee, S. E. J., R. A. O'Connor, I. Mair, M. D. Leech, A. Williams, and S. M. Anderton. 2017. IL-10-producing, ST2-expressing Foxp3$^+$ T cells in multiple sclerosis brain lesions. *Immunol. Cell Biol.* 95: 484–490.
20. Qi, Y., D. J. Operario, S. N. Georas, and T. R. Mosmann. 2012. The acute environment, rather than T cell subset pre-commitment, regulates expression of the human T cell cytokine amphiregulin. *PLoS One* 7: e39072.
21. Bowcutt, R., L. B. Malter, L. A. Chen, M. J. Wolff, I. Robertson, D. B. Rifkin, M. Poles, I. Cho, and P. Loke. 2015. Isolation and cytokine analysis of lamina propria lymphocytes from mucosal biopsies of the human colon. *J. Immunol. Methods* 421: 27–35.

22. Himmel, M. E., K. G. MacDonald, R. V. Garcia, T. S. Steiner, and M. K. Levings. 2013. Helios^{+} and Helios^{-} cells coexist within the natural FOXP3^{+} T regulatory cell subset in humans. *J. Immunol.* 190: 2001–2008.
23. Persson, H., W. Ye, A. Wernimont, J. J. Adams, A. Koide, S. Koide, R. Lam, and S. S. Sidhu. 2013. CDR-H3 diversity is not required for antigen recognition by synthetic antibodies. *J. Mol. Biol.* 425: 803–811.
24. Love, M. I., W. Huber, and S. Anders. 2014. Moderated estimation of fold change and dispersion for RNA-seq data with DESeq2. *Genome Biol.* 15: 550.
25. Subramanian, A., P. Tamayo, V. K. Mootha, S. Mukherjee, B. L. Ebert, M. A. Gillette, A. Paulovich, S. L. Pomeroy, T. R. Golub, E. S. Lander, and J. P. Mesirov. 2005. Gene set enrichment analysis: a knowledge-based approach for interpreting genome-wide expression profiles. *Proc. Natl. Acad. Sci. USA* 102: 15545–15550.
26. Fletcher, J. M., R. Lonergan, L. Costelloe, K. Kinsella, B. Moran, C. O'Farrelly, N. Tubridy, and K. H. Mills. 2009. CD39^{+}Foxp3^{+} regulatory T cells suppress pathogenic Th17 cells and are impaired in multiple sclerosis. *J. Immunol.* 183: 7602–7610.
27. Baecher-Allan, C., E. Wolf, and D. A. Hafler. 2006. MHC class II expression identifies functionally distinct human regulatory T cells. *J. Immunol.* 176: 4622–4631.
28. Joller, N., E. Lozano, P. R. Burkett, B. Patel, S. Xiao, C. Zhu, J. Xia, T. G. Tan, E. Sefik, V. Yajnik, et al. 2014. Treg cells expressing the coinhibitory molecule TIGIT selectively inhibit proinflammatory Th1 and Th17 cell responses. *Immunity* 40: 569–581.
29. Kurtulus, S., K. Sakuishi, S. F. Ngiow, N. Joller, D. J. Tan, M. W. Teng, M. J. Smyth, V. K. Kuchroo, and A. C. Anderson. 2015. TIGIT predominantly regulates the immune response via regulatory T cells. *J. Clin. Invest.* 125: 4053–4062.
30. Monticelli, L. A., G. F. Sonnenberg, M. C. Abt, T. Alenghat, C. G. Ziegler, T. A. Doering, J. M. Angelosanto, B. J. Laidlaw, C. Y. Yang, T. Sathaliyawala, et al. 2011. Innate lymphoid cells promote lung-tissue homeostasis after infection with influenza virus. *Nat. Immunol.* 12: 1045–1054.
31. Monticelli, L. A., L. C. Osborne, M. Noti, S. V. Tran, D. M. Zaiss, and D. Artis. 2015. IL-33 promotes an innate immune pathway of intestinal tissue protection dependent on amphiregulin-EGFR interactions. *Proc. Natl. Acad. Sci. USA* 112: 10762–10767.
32. Liu, X., M. Hammel, Y. He, J. A. Tainer, U. S. Jeng, L. Zhang, S. Wang, and X. Wang. 2013. Structural insights into the interaction of IL-33 with its receptors. *Proc. Natl. Acad. Sci. USA* 110: 14918–14923.
33. Mjösberg, J. M., S. Trifari, N. K. Crellin, C. P. Peters, C. M. van Drunen, B. Piet, W. J. Fokkens, T. Cupedo, and H. Spits. 2011. Human IL-25- and IL-33–responsive type 2 innate lymphoid cells are defined by expression of CRTH2 and CD161. *Nat. Immunol.* 12: 1055–1062.
34. Morita, H., K. Arae, H. Unno, K. Miyauchi, S. Toyama, A. Nambu, K. Oboki, T. Ohno, K. Motomura, A. Matsuda, et al. 2015. An interleukin-33-mast cell-interleukin-2 Axis suppresses papain-induced allergic inflammation by promoting regulatory T cell numbers. *Immunity* 43: 175–186.
35. Han, J. M., D. Wu, H. C. Denroche, Y. Yao, C. B. Verchere, and M. K. Levings. 2015. IL-33 reverses an obesity-induced deficit in visceral adipose tissue ST2^{+} T regulatory cells and ameliorates adipose tissue inflammation and insulin resistance. *J. Immunol.* 194: 4777–4783.
36. Vasanthakumar, A., K. Moro, A. Xin, Y. Liao, R. Gloury, S. Kawamoto, S. Fagarasan, L. A. Mielke, S. Afshar-Sterle, S. L. Masters, et al. 2015. The transcriptional regulators IRF4, BATF and IL-33 orchestrate development and maintenance of adipose tissue-resident regulatory T cells. *Nat. Immunol.* 16: 276–285.
37. Popovic, B., M. Golemac, J. Podlech, J. Zeleznjak, L. Bilic-Zulle, M. L. Lukic, L. Cicin-Sain, M. J. Reddehase, T. Sparwasser, A. Krmpotic, and S. Jonjic. 2017. IL-33/ST2 pathway drives regulatory T cell dependent suppression of liver damage upon cytomegalovirus infection. *PLoS Pathog.* 13: e1006345.
38. Wynn, T. A., and K. M. Vannella. 2016. Macrophages in tissue repair, regeneration, and fibrosis. *Immunity* 44: 450–462.
39. Taams, L. S., J. M. van Amelsfort, M. M. Tiemessen, K. M. Jacobs, E. C. de Jong, A. N. Akbar, J. W. Bijlsma, and F. P. Lafeber. 2005. Modulation of monocyte/macrophage function by human CD4+CD25+ regulatory T cells. *Hum. Immunol.* 66: 222–230.
40. Tiemessen, M. M., A. L. Jagger, H. G. Evans, M. J. van Herwijnen, S. John, and L. S. Taams. 2007. CD4+CD25+Foxp3+ regulatory T cells induce alternative activation of human monocytes/macrophages. *Proc. Natl. Acad. Sci. USA* 104: 19446–19451.
41. Nile, C. J., E. Barksby, P. Jitprasertwong, P. M. Preshaw, and J. J. Taylor. 2010. Expression and regulation of interleukin-33 in human monocytes. *Immunology* 130: 172–180.
42. Carney, K., Y. R. Chang, S. Wilson, C. Calnan, P. S. Reddy, W. Y. Chan, T. Gilmartin, G. Hernandez, L. Schaffer, S. R. Head, et al. 2016. Regulatory T-cell-intrinsic amphiregulin is dispensable for suppressive function. *J. Allergy Clin. Immunol.* 137: 1907–1909.
43. Green, J. A., N. Arpaia, M. Schizas, A. Dobrin, and A. Y. Rudensky. 2017. A nonimmune function of T cells in promoting lung tumor progression. *J. Exp. Med.* 214: 3565–3575.
44. Wu, D., J. M. Han, X. Yu, A. J. Lam, R. E. Hoeppli, A. M. Pesenacker, Q. Huang, V. Chen, C. Speake, E. Yorke, et al. 2018. Characterization of regulatory T cells in obese omental adipose tissue in humans. *Eur. J. Immunol.*
45. Siede, J., A. Fröhlich, A. Datsi, A. N. Hegazy, D. V. Varga, V. Holecska, H. Saito, S. Nakae, and M. Löhning. 2016. IL-33 receptor-expressing regulatory T cells are highly activated, Th2 biased and suppress CD4 T cell proliferation through IL-10 and TGFβ release. *PLoS One* 11: e0161507.
46. Turnquist, H. R., Z. Zhao, B. R. Rosborough, Q. Liu, A. Castellaneta, K. Isse, Z. Wang, M. Lang, D. B. Stolz, X. X. Zheng, et al. 2011. IL-33 expands suppressive CD11b^{+} Gr-1^{int} and regulatory T cells, including ST2L^{+} Foxp3^{+} cells, and mediates regulatory T cell-dependent promotion of cardiac allograft survival. *J. Immunol.* 187: 4598–4610.
47. Kolodin, D., N. van Panhuys, C. Li, A. M. Magnuson, D. Cipolletta, C. M. Miller, A. Wagers, R. N. Germain, C. Benoist, and D. Mathis. 2015. Antigen- and cytokine-driven accumulation of regulatory T cells in visceral adipose tissue of lean mice. *Cell Metab.* 21: 543–557.
48. Chen, C. C., T. Kobayashi, K. Iijima, F. C. Hsu, and H. Kita. 2017. IL-33 dysregulates regulatory T cells and impairs established immunologic tolerance in the lungs. *J. Allergy Clin. Immunol.* 140: 1351–1363.e7.
49. Schmitz, J., A. Owyang, E. Oldham, Y. Song, E. Murphy, T. K. McClanahan, G. Zurawski, M. Moshrefi, J. Qin, X. Li, et al. 2005. IL-33, an interleukin-1-like cytokine that signals via the IL-1 receptor-related protein ST2 and induces T helper type 2-associated cytokines. *Immunity* 23: 479–490.
50. Jackson, D. J., H. Makrinioti, B. M. Rana, B. W. Shamji, M. B. Trujillo-Torralbo, J. Footitt, J. del-Rosario, A. G. Telcian, A. Nikonova, J. Zhu, et al. 2014. IL-33–dependent type 2 inflammation during rhinovirus-induced asthma exacerbations in vivo. *Am. J. Respir. Crit. Care Med.* 190: 1373–1382.
51. Seidelin, J. B., J. T. Bjerrum, M. Coskun, B. Widjaya, B. Vainer, and O. H. Nielsen. 2010. IL-33 is upregulated in colonocytes of ulcerative colitis. *Immunol. Lett.* 128: 80–85.
52. Pastorelli, L., R. R. Garg, S. B. Hoang, L. Spina, B. Mattioli, M. Scarpa, C. Fiocchi, M. Vecchi, and T. T. Pizarro. 2010. Epithelial-derived IL-33 and its receptor ST2 are dysregulated in ulcerative colitis and in experimental Th1/Th2 driven enteritis. *Proc. Natl. Acad. Sci. USA* 107: 8017–8022.
53. Kobori, A., Y. Yagi, H. Imaeda, H. Ban, S. Bamba, T. Tsujikawa, Y. Saito, Y. Fujiyama, and A. Andoh. 2010. Interleukin-33 expression is specifically enhanced in inflamed mucosa of ulcerative colitis. *J. Gastroenterol.* 45: 999–1007.
54. MacDonald, K. G., N. A. Dawson, Q. Huang, J. V. Dunne, M. K. Levings, and R. Broady. 2015. Regulatory T cells produce profibrotic cytokines in the skin of patients with systemic sclerosis. *J. Allergy Clin. Immunol.* 135: 946–955.e9.
55. University of Leicester; Leicester Respiratory Biomedical Research Centre, Glenfield Hospital; Leicester Clinical Trials Unit; Genentech, Inc. 2018. Anti-ST2 (MSTT1041A) in COPD (COPD-ST2OP) (COPD-ST2OP). In: ClinicalTrials.gov. National Library of Medicine (US), Bethesda, MD. NLM Identifier: NCT03615040. Available at: https://clinicaltrials.gov/ct2/show/NCT03615040. Accessed: August 15, 2018.
56. GlaxoSmithKline. 2017. Efficacy and safety study of GSK3772847 in subjects with moderately severe asthma. In: ClinicalTrials.gov. National Library of Medicine (US), Bethesda, MD. NLM Identifier: NCT03207243. Available at: https://clinicaltrials.gov/ct2/show/NCT03207243. Accessed: August 15, 2018.
57. GlaxoSmithKline. 2018. Repeat dose study of GSK3772847 in participants with moderate to severe asthma with allergic fungal airway disease (AFAD). In: ClinicalTrials.gov. National Library of Medicine (US), Bethesda, MD. NLM Identifier: NCT03393806. Available at: https://clinicaltrials.gov/ct2/show/NCT03393806. Accessed: August 15, 2018.
58. Povoleri, G. A. M., E. Nova-Lamperti, C. Scottà, G. Fanelli, Y. C. Chen, P. D. Becker, D. Boardman, B. Costantini, M. Romano, P. Pavlidis, et al. 2018. Human retinoic acid-regulated CD161^{+} regulatory T cells support wound repair in intestinal mucosa. *Nat. Immunol.* 19: 1403–1414.